



# INTERNATIONAL JOURNAL OF COMPUTERS AND THEIR APPLICATIONS

---

## TABLE OF CONTENTS

	Page
<b>New Superfast Bit Reversal Algorithms on Uniprocessors</b> .....	147
<i>Rami A. Al Na'mneh and Khalid A. Darabkh</i>	
<b>A Study of the Performance of Diversity Combining Schemes on Multipath Fading at 900MHz</b> .....	157
<i>A. J. Falade</i>	
<b>A Personal Identification System Based on Iris Recognition</b> .....	164
<i>Khalid A. Buragga, Sultan Aljahdali, Ahmad. M. Sarhan and Marcel Karam</i>	
<b>Using Genetic Algorithm &amp; Neural Network for Modeling Learning Behavior in a Multi-Agent System during Emergency Evacuation</b> .....	172
<i>Sharad Sharma and Kolawole Ogunlana</i>	
<b>Index</b> .....	183

\* "International Journal of Computers and Their Applications is abstracted and indexed in INSPEC and Scopus."

# International Journal of Computers and Their Applications

*A publication of the International Society for Computers and Their Applications*

## EDITOR-IN-CHIEF

Dr. Frederick C. Harris, Jr., Professor  
Department of Computer Science and Engineering  
University of Nevada, Reno, NV 89557, USA  
Phone: 775-784-6571, Fax: 775-784-1877  
Email: Fred.Harris@cse.unr.edu, Web: <http://www.cse.unr.edu/~fredh>

## ASSOCIATE EDITORS

**Dr. Hisham Al-Mubaid**  
University of Houston-Clear Lake,  
USA  
hisham@uhcl.edu

**Dr. Antoine Bossard**  
Advanced Institute of Industrial  
Technology, Tokyo, Japan  
abossard@aiit.ac.jp

**Dr. Mark Burgin**  
University of California,  
Los Angeles, USA  
mburgin@math.ucla.edu

**Dr. Sergiu Dascalu**  
University of Nevada, USA  
dascalus@cse.unr.edu

**Dr. Sami Fadali**  
University of Nevada, USA  
fadali@ieee.org

**Dr. Vic Grout**  
Glyndŵr University,  
Wrexham, UK  
v.grout@glyndwr.ac.uk

**Dr. Yi Maggie Guo**  
University of Michigan,  
Dearborn, USA  
magyiguo@umich.edu

**Dr. Wen-Chi Hou**  
Southern Illinois University, USA  
hou@cs.siu.edu

**Dr. Ramesh K. Karne**  
Towson University, USA  
rkarne@towson.edu

**Dr. Bruce M. McMillin**  
Missouri University of Science and  
Technology, USA  
ff@mst.edu

**Dr. Muhanna Muhanna**  
Princess Sumaya University for  
Technology, Amman, Jordan  
m.muhanna@psut.edu.jo

**Dr. Mehdi O. Owrang**  
The American University, USA  
owrang@american.edu

**Dr. Xing Qiu**  
University of Rochester, USA  
xqiu@bst.rochester.edu

**Dr. Abdelmounaam Rezgui**  
New Mexico Tech, USA  
rezgui@cs.nmt.edu

**Dr. James E. Smith**  
West Virginia University, USA  
James.Smith@mail.wvu.edu

**Dr. Shamik Sural**  
Indian Institute of Technology  
Kharagpur, India  
shamik@cse.iitkgp.ernet.in

**Dr. Ramalingam Sridhar**  
The State University of New York at  
Buffalo, USA  
rsridhar@buffalo.edu

**Dr. Junping Sun**  
Nova Southeastern University, USA  
jps@nsu.nova.edu

**Dr. Jianwu Wang**  
University of California  
San Diego, USA  
jianwu@sdsc.edu

**Dr. Yiu-Kwong Wong**  
Hong Kong Polytechnic University,  
Hong Kong  
eeykwong@polyu.edu.hk

**Dr. Rong Zhao**  
The State University of New York  
at Stony Brook, USA  
rong.zhao@stonybrook.edu

ISCA Headquarters ••••• 64 White Oak Court, Winona, MN 55987 ••••• Phone: (507) 458-4517  
E-mail: [isca@ipass.net](mailto:isca@ipass.net) • URL: <http://www.isca-hq.org>

Copyright © 2015 by the International Society for Computers and Their Applications (ISCA)  
All rights reserved. Reproduction in any form without the written consent of ISCA is prohibited.

# New Superfast Bit Reversal Algorithms on Uniprocessors

Rami A. Al Na'mneh\*

Jordan University of Science and Technology, Irbid, 22110, JORDAN

Khalid A. Darabkh\*

The University of Jordan, Amman, 11942, JORDAN

## Abstract

Bit-reversal is a major step in Fast Fourier Transforms (FFT) and Fast Hartley Transform (FHT). Image transposition and generalized sorting of multidimensional arrays are other interesting applications of bit-reversal algorithms. In this paper, we propose two effective bit-reversal permutation algorithms, namely hierarchy transpose and swapping algorithms, that have a time complexity of  $O(\sqrt{n})$ . The *Elster* algorithm, one of the fastest available bit-reversal permutation algorithms, has a minimum time complexity of  $O(n)$ . Moreover, the hierarchy transpose and swapping algorithms

perform  $1.5n - 0.5\sqrt{n} - n^{\frac{3}{4}}$  and  $n - n^{\frac{3}{4}}$  swaps (or exchanges), respectively, which are lower than the transpose

algorithm that performs  $2n - n^{\frac{3}{4}}$  exchanges. We use a look-up table of size  $\sqrt{n}$  to perform the bit-reversal experimentally. The results show that our proposed algorithms outperform the *Elster* algorithm for small data sizes. On the other hand, the results show that the swapping algorithm is the best among the transpose and hierarchy transpose algorithms. Our experimental results have been theoretically validated. Furthermore, our proposed algorithms can be used efficiently in parallel systems since they consist of parallelizable steps.

**Key Words:** Bit-reversal, performance analysis, time complexity, fast Fourier transforms, hierarchy transpose and swapping algorithms.

## 1 Introduction

The Discrete Fourier Transform (DFT) has wide applications in science and engineering whereas many Fast Fourier Transform algorithms (FFT) have been proposed to enhance the computing of DFT through achieving a significant decrease in its computational time [3, 7]. Moreover, the FFT helps much in simplifying the required analysis for physics, astronomy, cryptography, as well as computational finance [2].

It was originally developed by J. W. Cooley and J. W. Tukey in 1965 [8]. Thereafter, new FFT algorithms were proposed, which mainly include milestone improvements, such as split-radix algorithms [11], mixed-radix algorithms [28], prime factor algorithms [6], and multidimensional FFT algorithms [19]. The FFT can be classified into two classes, decimation in frequency and decimation in time [2, 7]. The bit-reversal step of FFT is the last stage in decimation in frequency and the first stage in decimation in time [14, 18, 25, 30]. Bit-reversal operation of the FFT takes a significant amount of the workload of the entire FFT computation [25, 30]. For example, in a length of 1024 split radix FFT, the bit-reversal requires about 20% of the time needed to perform the FFT itself [10].

There are many research articles which efficiently implement bit-reversal algorithms in a single computer [5, 9-10, 12-13, 15-16, 22, 24, 26, 31-33]. Some of these papers focus on reducing the number of needed operations [9-10, 22, 26, 12-13, 15-16, 31-32] (i.e., additions, multiplications, etc.) while others focus on optimizing the memory hierarchy (i.e., caches, translation-lookaside buffer (TLB), and memory), out of which techniques such as blocking, buffering, and padding were employed and, accordingly, examined to be cache and TLB effective [5, 17, 33]. Additionally, it is noteworthy to mention that those articles that have the interest of reducing the number of operations can be further classified into two classes: the first class involves implementing the bit-reversal using auxiliary table (*seed* table) of size  $\sqrt{n}$  [10, 13, 15, 22, 24, 31] if  $n = 2^{2a}$  or  $\sqrt{n/2}$  if  $n = 2^{2a+1}$ , where  $n$  is the length of the transform and  $a$  is the length of the binary expansion of an index  $i$ . For example, in [24], the authors succeeded in reducing the number of required loops using the property of symmetry but along with the use of look-up tables lead eventually to wasting on a lot of memory space. The authors in [22] reported that the bit-reversal can be done adeptly using vectors rather than loops by finding the bit-reversal of elements one after another. Nonetheless, this method works fine in programming environments that offer algorithms that deal more efficiently with vectors than loops like Matlab. The look-up table used contains a pre-computed matrix vector multiplication. However, the second class does not use *seed* tables in implementing the bit-reversal [9, 12, 22, 26]. For example, the author in [32] proposed a heuristic

\* Department of Computer Engineering. E-mail: {ramir11@just, k.darabkeh@ju}.edu.jo. Phone #: +962-796969219. Fax: +962-65300813.

approach that repeats only  $\frac{n}{4}$  times instead of  $n$  times in loops as widely explored in the literature. In [26], the authors proposed an algorithm based on a pseudo semi-group homomorphism property that has a complexity of  $O(n)$ . However, it is proven that the algorithms of the first class run much faster than those found in the second class except for some cases described in [18].

In summary, all of the above proposed bit-reversal algorithms were implemented in different ways which may need various steps to get them done such as  $O(n \log n)$  steps [33] and  $O(n)$  steps [12, 24, 32]. Hence, among these algorithms, the best of them requires at least  $O(n)$  operations. A summary of 30 methods that compute the bit-reversals are reported by [20]. Among these methods, the *Elster* method proposed in [12] was found the fastest. As a further evidence of its importance, it has been used by [13] to come up with a new version suitable for modern multithreaded architectures, whereas it has been proven that a minimally tuned Cooley-Tukey FFT using that modified bit-reversal version performs better than the default FFTW algorithm. Further details about FFTW are found in [16].

In this paper, we propose two bit-reversal permutation algorithms; namely, hierarchy transpose and swapping algorithms. We assume that the array of size  $n$  can be represented as  $\sqrt{n} \times \sqrt{n}$  array. However, the first permutation algorithm is an extension to the transpose algorithm proposed in [22]. As reported in [22], the transpose algorithm consists of three steps: find the bit-reversal for just the first row, transpose the array, and then repeat the first step. The first proposed permutation algorithm utilizes the same first and last steps of the transpose algorithm but it uses a more efficient transpose algorithm and this is done to show the impact of transposing the array on the whole bit-reversal time. The other proposed permutation algorithm consists of two steps: find the bit-reversal for the first row and then for the first column. It is good to point out that we do not swap elements one after another as any available bit-reversal algorithms, but rather we swap vector with vector which consequently saves time. As mentioned before, the *Elster* algorithm, which is considered one of the best algorithms to compute the bit-reversal, using data inputs of size  $n$  has a time complexity of  $O(n)$ , whereas

our algorithms have the time complexity  $O(\sqrt{n})$ . On the other hand, the *Elster* algorithm performs  $\frac{1}{2}(n - n^2)$  exchanges while our hierarchy transpose and swapping algorithms perform  $1.5n - 0.5\sqrt{n} - n^{\frac{3}{4}}$  and  $n - n^{\frac{3}{4}}$  swaps, respectively. These are undoubtedly lower than what are required for the transpose algorithm which is  $2n - n^{\frac{3}{4}}$  exchanges. (b)The ability of

applying our proposed ideas to enhance current bit-reversal algorithms is feasible. Additionally, our proposed algorithms are faster than the *Elster* algorithm for small data inputs and transpose algorithm for all data sizes. Hence, it is highly recommended to use them within this capacity of data inputs. Furthermore, they consist of independent tasks in which they can be easily and efficiently parallelized. As a matter of fact, preliminary results of this work have been presented in [1].

The rest of the paper is organized as follows. In Section 2, the idea of bit-reversal along with a detailed description of a relevant bit-reversal algorithm called the transpose algorithm are provided. In Section 3, our proposed bit-reversal algorithms are presented and extensively detailed. Section 4 includes the performance analysis for our proposed algorithms along with the transpose and *Elster* algorithms. Experimental results and discussion are presented in Section 5. Finally, the paper is concluded in Section 6.

## 2 Bit-Reversal Permutations

### 2.1 The Idea of Bit-Reversal

The idea of finding the bit-reversal is based on the following discussion: if we want to find the bit-reversal for any binary number, we can divide this number into two parts (right and left). Then, we find the bit-reversal for each side separately. Next, we swap both sides to obtain eventually the bit-reversal. For example, if we want to find the bit-reversal for 34 (100010), we divide the number into two parts, right=100 and left =010. We find the bit-reversal for the right side, which is 001 and for the left side, which is 010. Then, we swap the right and the left, to get finally 010001.

### 2.2 The Transpose Algorithm

The transpose algorithm was proposed in [22]. In order to find the bit-reversal of a data of size  $n$ , they save the original data in a two-dimensional array of size  $(\sqrt{n} \times \sqrt{n})$  as shown in Figure 1(a). Figure 1 is done to illustrate how to perform the bit-reversal for data inputs of size 64 (i.e.,  $n=64$ ) using this algorithm. However, each index of the array is thus a concatenation of the row index and column index. To this end, the following steps are taken for simulating this algorithm:

1. Finding the bit-reversal for the column-index of the first row. Consequently, they swap these indices, but in order to save time, the whole column is swapped with its bit-reversed column, as shown in Figure 1(b), instead of swapping pairs of indices.
2. Transposing the matrix in a way that the row becomes column and vice versa as shown in Figure 1(c). In their implementation, they used out of place arrays, that are two different arrays, to transpose all elements of the matrix. The cost to do this copy is  $O(n)$ , where each matrix used is of size  $n$ . On the other hand, there are

000	001	010	011	100	101	110	111
0	1	2	3	4	5	6	7
8	9	10	11	12	13	14	15
16	17	18	19	20	21	22	23
24	25	26	27	28	29	30	31
32	33	34	35	36	37	38	39
40	41	42	43	44	45	46	47
48	49	50	51	52	53	54	55
56	57	58	59	60	61	62	63

(a) The original data is set into two-dimensional array  $(\sqrt{n} \times \sqrt{n})$

000	001	010	011	100	101	110	111
0	4	2	6	1	5	3	7
8	12	10	14	9	13	11	15
16	20	18	22	17	21	19	23
24	28	26	30	25	29	27	31
32	36	34	38	33	37	35	39
40	44	42	46	41	45	43	47
48	52	50	54	49	53	51	55
56	60	58	62	57	61	59	63

(b) The results after finding the bit-reversal for the column-index of the first row and swapping each column with its bit-reversed column

000	001	010	011	100	101	110	111
0	8	16	24	32	40	48	56
4	12	20	28	36	44	52	60
2	10	18	26	34	42	50	58
6	14	22	30	38	46	54	62
1	9	17	25	33	41	49	57
5	13	21	29	37	45	53	61
3	11	19	27	35	43	51	59
7	15	23	31	39	47	55	63

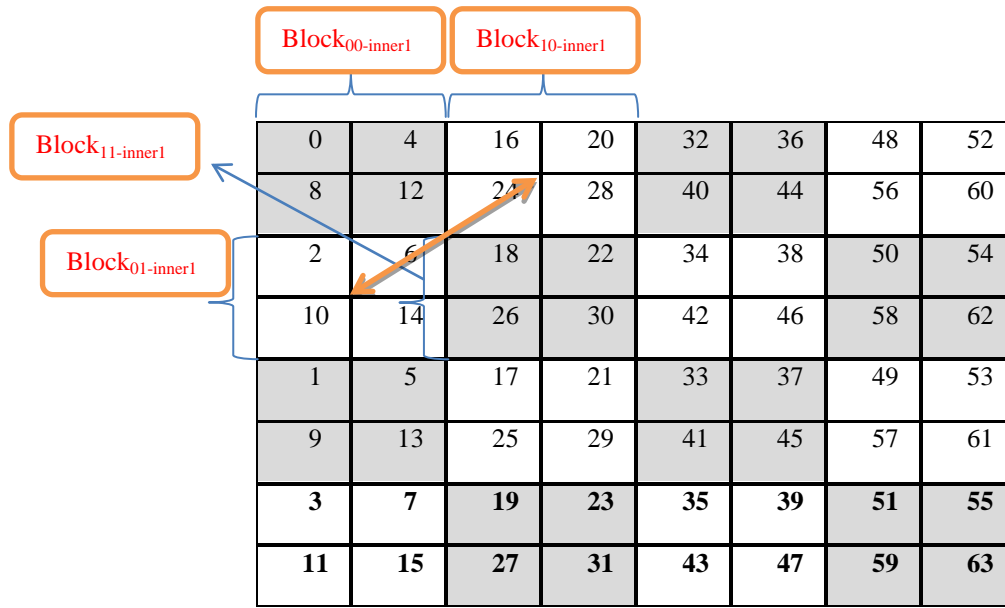
(c) The results after the array is transposed

000	001	010	011	100	101	110	111
0	32	16	48	8	40	24	56
4	36	20	52	12	44	28	60
2	34	18	50	10	42	26	58
6	38	22	54	14	46	30	62
1	33	17	49	9	41	25	57
5	37	21	53	13	45	29	61
3	35	19	51	11	43	27	59
7	39	23	55	15	47	31	63

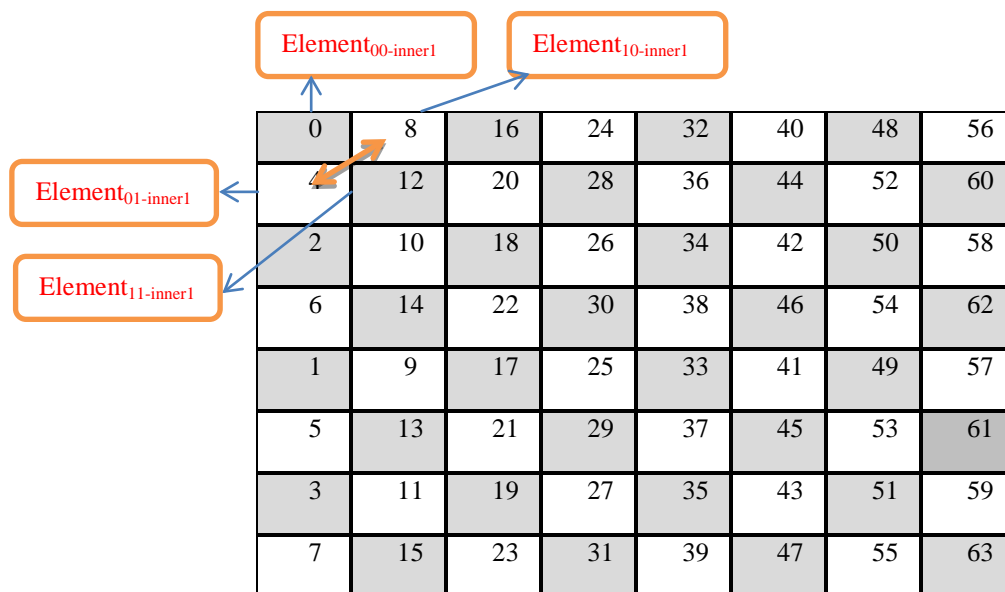
(d) The results after finding the bit-reversal for the column-index of the first row and swapping each column with its bit-reversed column considering the matrix was transposed

Figure 1(a, b, c, and d): An example of how to perform the bit-reversal for data inputs of size 64 using the transpose algorithm





b. The 8x8 matrix after swapping the outer (block<sub>i,j-outer</sub>) and inner (block<sub>i,j-inner1</sub>) blocks such that  $i \neq j$



c. The final results after transposing the 8x8 matrix using hierarchy transpose where the elements inside the inner blocks are swapped

Figure 2(a, b, and c): Description of the hierarchy transpose algorithm

	000	001	010	011	100	101	110	111
0	0	8	16	24	32	40	48	56
1	1	9	17	25	33	41	49	57
2	2	10	18	26	34	42	50	58
3	3	11	19	27	35	43	51	59
4	4	12	20	28	36	44	52	60
5	5	13	21	29	37	45	53	61
6	6	14	22	30	38	46	54	62
7	7	15	23	31	39	47	55	63

(a) The input data n is set in two-dimensional array  $(\sqrt{n} \times \sqrt{n})$

	000	001	010	011	100	101	110	111
0	0	32	16	48	8	40	24	56
1	1	33	17	49	9	41	25	57
2	2	34	18	50	10	42	26	58
3	3	35	19	51	11	43	27	59
4	4	36	20	52	12	44	28	60
5	5	37	21	53	13	45	29	61
6	6	38	22	54	14	46	30	62
7	7	39	23	55	15	47	31	63

(b) The results after finding the bit-reversal for the column-index of first row and swap each column with its bit-reversed column

	000	001	010	011	100	101	110	111
000	0	32	16	48	8	40	24	56
001	4	36	20	52	12	44	28	60
010	2	34	18	50	10	42	26	58
011	6	38	22	54	14	46	30	62
100	1	33	17	49	9	41	25	57
101	5	37	21	53	13	45	29	61
110	3	35	19	51	11	43	27	59
111	7	39	23	55	15	47	31	63

(c) The results after finding the bit-reversal for the row-index of the first column, but this time we swap the whole row with the corresponding bit-reversed row

Figure 3(a, b, and c): An example of performing the bit-reversal using the swapping algorithm for an input data of size 64

that our proposed algorithms are totally correct since they validate each other.

Procedure 1 describes the pseudo code used to simulate the last step of this proposed algorithm. In this pseudo code, we use a look-up table to find the corresponding bit-reversal for each index of the original data vector. If the bit-reversal of the index is the same as the index, we just do nothing. Otherwise, we should swap the whole row with its corresponding bit-reversed row.

#### Procedure I – Pseudo code to simulate step three of the third proposed algorithm

**IN:** input data vector  $n$

**OUT:** two-dimensional array (Data)

**begin**

$i = 0;$

$j = 0;$

$k = 0;$

**While** ( $i < \sqrt{n}$ ) **do**

**Begin**

$j = \text{bit reversal}(i)$  //get the bit-reversal using look-up

table

**if**  $j < i$  **then**

$\text{Temp} = 0;$

**While** ( $k < \sqrt{n}$ ) **do**

corresponding bit-reversed rows

$\text{Temp} = \text{Data}(i)(k);$

$\text{Data}(i)(k) = \text{Data}(j)(k);$

$\text{Data}(j)(k) = \text{Temp};$

          Increment  $k;$

**end while**

**endif**

      Increment  $i;$

**end while**

**end**

#### 4 Performance Analysis

It is interesting to investigate the significance of our conclusions in this paper by conducting a performance analysis for our proposed bit-reversal algorithms and then making comparisons between them and the transpose algorithm along with one of the most popular bit-reversal algorithms, namely the *Elster* algorithm, considering small and large input data sizes given that the bit-reversal step in the computation of the FFT comprises a significant portion of the FFT computational time. However, if we assume that the size of the input vector is  $n = \sqrt{n} \times \sqrt{n}$ , then the analysis for the proposed algorithms can be summarized as follows:

To make the evaluation of our proposed algorithms effective and clear, analysis for the transpose algorithm was conducted because it had not been included in [22]. However, the first and last steps of the transpose algorithm are to find the bit-reversal for the column indices of the first rows where each row is of size  $\sqrt{n}$  and then swap each column with its

corresponding bit-reversed column, as shown in Figure 1(b) and (d), respectively. Consequently, the time complexity of finding the bit-reversal for these steps is expressed as:

$$T_{Transpose\_bit\_reversal} = 2\sqrt{n}. \quad (1)$$

where  $\sqrt{n}$  is considered for each step. It is worth mentioning that the complexity includes an addition and a comparison in each iteration of a loop bounded by  $\sqrt{n}$ . However, when considering the big-O notation, the time complexity of this algorithm is  $O(\sqrt{n})$ . On the other hand, the *Elster* algorithm has a time complexity of:

$$T_{Elster\_bit\_reversal} = n. \quad (2)$$

which includes a shift and XOR in each iteration of a loop consisting of  $n$  iterations. At present, it is very important to find the number of swaps performed in the transpose algorithm. In the *Elster* algorithm, the number of swaps performed is:

$$N_{Elster\_swaps} = \frac{n - n^{\frac{1}{2}}}{2}. \quad (3)$$

for input data of size  $n$  [13]. Hence, in the first and last steps of the transpose algorithm, the number of swaps ( $N_{swaps}$ ) can be expressed as:

$$N_{Transpose\_FLS\_swaps} = 2\sqrt{n} \left( \frac{\sqrt{n} - n^{\frac{1}{4}}}{2} \right) = n - n^{\frac{3}{4}}. \quad (4)$$

Considering Step 2 of the transpose algorithm, which indicates making a transpose for the two-dimensional array, it is worth mentioning that the number of exchanges, which involve load and store operations, needed is  $n$  if the transpose is done out of place (i.e., using two 2D arrays) [22]. Therefore, we can declare that the total number of swaps operations required for the transpose algorithm ( $N_{overall\_swaps}$ ) is:

$$N_{Transpose\_overall\_swaps} = 2n - n^{\frac{3}{4}}. \quad (5)$$

On the other hand, in our first proposed algorithm (hierarchy transpose algorithm), we use an efficient transpose algorithm that is carried out in place, as extensively explained in Section 3 of this paper which has a number of exchanges  $(n - \sqrt{n})/2$ . Therefore,  $N_{overall\_swaps}$  is improved for the hierarchy transpose algorithm as follows:

$$N_{HT\_overall\_swaps} = 1.5n - 0.5\sqrt{n} - n^{\frac{3}{4}}. \quad (6)$$

As far as the second proposed algorithm (swapping algorithm) is concerned, we can notice that the time complexity of its Step 2 is the same as the one just explained for Step 1 of the transpose algorithm. On the other hand, Step 3 in the swapping algorithm has the time complexity of  $\sqrt{n}$  steps, as shown in procedure 1, the loop is repeated  $\sqrt{n}$  times. In this step, instead of performing the bit-reversal for each column, we swap the whole row with its corresponding bit-reversed row after finding the bit-reversal of the row-index of the first column. Therefore, the time complexity of this step is  $\sqrt{n}$ . Hence, the overall time complexity is:

$$T_{Swapping\_bit\_reversal} = 2\sqrt{n}. \quad (7)$$

The number of swaps needed for steps 2 and 3 is:

$$N_{Swapping\_overall\_swaps} = n - n^{\frac{3}{4}}. \quad (8)$$

In each step of the proposed algorithms concerning the way of obtaining the bit-reversal, we use a look-up table to get the bit-reversal value of the corresponding array index.

## 5 Results and Discussion

For the sake of evaluating our proposed algorithms over the well-known sequential bit-reversal algorithms, namely, the *Elster* and transpose algorithms, we simulate the *Elster*, transpose, and our proposed algorithms on Pentium 4 2.4 GHz with 512k cache and 256MB DDR-SDRAM. The software configuration environment used is as follows: Redhat 7.3 Operating system, Kernel 2.4.18, as well as gcc compiler. The size of input vector varied between 16 (4x4) and 1048576 (1024x1024) of data. In order to get accurate results, we run the code 10000 times for each data size. The obtained results

are shown in Table 1.

It is noticed, in all algorithms, the increase in bit-reversal time as the data size increases and this is due to having larger elements in the 2D array which requires more iterations and swaps. The results of our proposed algorithms outperform those obtained from the transpose algorithm. This is to be expected since the number of swaps in our proposed algorithms is always less. It is worth mentioning that the time required to find the bit-reversal using our proposed algorithms is lower than that using the *Elster* algorithm for small data sizes. This is expected in light of our detailed performance analysis since the number of swaps for all proposed algorithms is not the dominant factor as long as the employed data sizes are small, but rather it is the bit-reversal time (either for the row-index or column-index of a 2D array as described in Sections 2 and 3), whereas it is completely the opposite as the data sizes increases drastically. For example, the overall time to do the bit-reversal, when the data size is 4x4, is 0.2501, 0.388622, 0.2432, and 0.1192 for the transpose, *Elster*, hierarchy transpose, and swapping algorithms, respectively. While these values, when the data size is 1024x1024, are 43723, 28013, 41675, and 35723, respectively. When comparing the number of swaps required for the *Elster* algorithm and our proposed algorithms through taking the limit of the input data size ( $n$ ) as it goes to infinity to denote for very larger data size, we can first obtain the following ratio of swaps between the second proposed (swapping) algorithm and *Elster* algorithm:

$$Ratio_1 = \lim_{n \rightarrow \infty} \frac{\frac{1}{n-n^2}}{\frac{2}{n-n^{\frac{3}{4}}}} \approx \frac{1}{2} \quad (9)$$

This ratio is increased for the transpose and hierarchy transpose algorithms due to the effect of transposing the array. It is particularly observed when substituting equations (5) and (6) into the denominator of equation (9). It is about 0.25 and 0.33 for the transpose and hierarchy transpose algorithms, respectively. From these values of the limit ratio (i.e., 0.25 for

Table 1: Time comparison (in micro-second) between our proposed algorithms, transpose algorithm, and *Elster* algorithm for different data sizes

Data size	Transpose algorithm [18]	<i>Elster</i> algorithm [19]	Hierarchy Transpose algorithm (first proposed)	Swapping algorithm (second proposed)
<b>4x4</b>	0.2501	0.388622	0.2432	<b>0.1192</b>
<b>8x8</b>	0.83903	1.18017	0.7786	<b>0.4982</b>
<b>16x16</b>	4.251	4.59909	3.987	<b>2.361</b>
<b>32x32</b>	18.11	18.658	17.34	<b>11.229</b>
<b>64x64</b>	87.862	74.7395	85.23	<b>52.118</b>
<b>128x128</b>	353.84	329.48	325.56	<b>205.829</b>
<b>256x256</b>	1498	1320	1450	<b>1402</b>
<b>512x512</b>	8235	6937	7986	<b>7321</b>
<b>1024x1024</b>	<b>43723</b>	<b>28013</b>	<b>41675</b>	<b>35723</b>

the transpose algorithm, 0.33 for the hierarchy transpose algorithm, as well as 0.5 for the swapping algorithm), we can theoretically state that the best proposed algorithm is the swapping algorithm. This can be verified experimentally in the obtained results. As shown in Table 1, it is the fastest of not only the transpose and hierarchy transpose algorithms, but also the *Elster* algorithm as long as the data sizes are less than or equal 128x128 while the transpose and hierarchy transpose algorithms outperform the *Elster* algorithm as long as the data sizes are less than or equal 32x32, which is quite lower than that achieved in the swapping algorithm.

### 6 Concluding Remarks

Fast Fourier Transform plays a vital role in a wide range of applications such as telecommunications, image and digital signal processing, convolution, particle simulation, as well as weather forecasting. On the other hand, the bit-reversal step in the computation of the FFT comprises a significant portion of this time. In our proposed work, the experimentations revealed that the percentage of the sequential computational time of bit-reversal is between 15% - 30% of the total time of FFT. In fact, these values can be related to two causes: data size and how caches and memory hierarchies are used in the implementation. Due to its importance, we propose in this paper two efficient bit-reversal algorithms. These algorithms are compared with the *Elster* algorithm that has  $O(n)$  time complexity while our proposed algorithms have a time complexity of  $O(\sqrt{n})$ . The experimental results show that our proposed algorithms outperform the *Elster* algorithm for small employed data sizes. Once the data inputs become so large, the amount of exchanges or swaps needed for our proposed algorithms increases and becomes severely affected. Furthermore, our proposed algorithms outperform the transpose algorithm proposed in [22] for all data sizes. On the other hand, the results show that our swapping algorithm is the fastest among the transpose and hierarchy transpose algorithms and sustain more for larger operated data sizes. Additionally, our proposed algorithms can be implemented over any type of parallel systems efficiently such as symmetric multiprocessor systems or massively parallel processors.

### References

- [1] R. A. Al Na'mneh and K. A. Darabkh, "An Efficient Bit Reversal Permutation Algorithm," *Proceedings of 2013 IEEE International Conference on Robotics, Biomimetics, Intelligent Computational Systems (ROBIONETICS 2013)*, pp. 121-124, Yogyakarta, Indonesia, November 2013.
- [2] R. A. Al-Na'mneh and W. D. Pan, "Five-Step FFT Algorithm with Reduced Computational Complexity," *Information Processing Letters*, 101(6):262-267, March 2007.
- [3] R. A. AL-Na'mneh, W. D. Pan, and S.-M. Yoo, "Parallel Implementation of 1-D Fast Fourier Transform without Inter-Processor Communication," *International Journal of Computers and Applications*, 29(2):1-7, 2007.
- [4] J. Bruck, C. Ho, S. Kipnis, E. Upfal, and D. Weathersby, "Efficient Algorithms for All-to-All Communications in Multi-Port Message-Passing Systems," *IEEE Transactions on Parallel and Distributed Systems*, 8(11):1143-1156, November 1997.
- [5] L. Carter and K. Gatlin, "Towards an Optimal Bit-Reversal Permutation Program," *Proceedings of 39<sup>th</sup> Annual Symposium on Foundations of Computer Science*, pp. 544-553, Palo Alto, California, USA, November 1998.
- [6] S. C. Chan and K. L. Ho, "On Indexing the Prime Factor Fast Fourier Transform Algorithm," *IEEE Transactions on Circuits and Systems*, 38(8):951-953, August 1991.
- [7] W. T. Cochran, J. W. Cooley, D. L. Favon, H. D. Helms, R. A. Kaenel, W. W. Lang, G. C. Maling, D. E. Nelson, C. M. Rader, and P. D. Welch, "What is the Fast Fourier Transform?" *IEEE Transaction on Audio Electro Acoustics*, AU-15:45-55, June 1967.
- [8] J. W. Cooley and J. W. Tukey, "An Algorithm for the Machine Computation of the Complex Fourier Series," *Mathematics Computation*, 19:297-301, April 1965.
- [9] K. Drouiche, "A New Efficient Computational Algorithm for Bit Reversal Mapping," *IEEE Transactions on Signal Processing*, 49(1):251-254, January 2001.
- [10] P. Duhamel, "A Connection between Bit Reversal and Matrix Transposition: Hardware and Software Consequences," *IEEE Transactions on Signal Processing*, 38(11):1893-1896, November 1990.
- [11] P. Duhamel and H. Hollmann, "Split-Radix FFT Algorithm," *Electronic Letters*, 20:14-16, January 1984.
- [12] A. Elster, "Fast Bit-Reversal Algorithms," *Proceedings of IEEE International Conference on Acoustics, Speech, and Signal Processing 1989 (ICASSP'89)*, 2:1099-1102, Glasgow, Scotland, UK, May 1989.
- [13] A. Elster and J. Meyer, "A Super-Efficient Adaptable Bit-Reversal Algorithm for Multithreaded Architectures," *Proceedings of 23<sup>rd</sup> IEEE International Symposium on Parallel and Distributed Processing (IPDPS 2009)*, pp. 1-8, Rome, Italy, May 2009.
- [14] D. Evans, "An Improved Digital-Reversal Permutation Algorithm for the Fast Fourier Transforms," *IEEE Transactions on Acoustics, Speech, Signal Processing*, ASSP-35:1120-1125, August 1987.
- [15] D. M. W. Evans, "A Second Improved Digital-Reversal Permutation Algorithm for Fast Transforms," *IEEE Transactions on Acoustics, Speech, Signal Processing*, 37(8):1288-1291, August 1989.
- [16] M. Frigo, and S. G. Johnson, "The Design and Implementation of FFTW3," *Proceedings of the IEEE*, 93(2):216-231, February 2005.
- [17] L. K. Gatlin and L. Carter, "Memory Hierarchy Considerations for Fast Transpose and Bit-Reversals," *Proceedings of the Fifth International Symposium On High-Performance Computer Architecture*, pp. 33-42, Orlando, Florida, USA, January 1999.
- [18] B. Gold and B. Rader, *Digital Processing of Signal*, Mc-

Graw-Hill, New York, 1969.

- [19] A. Guessoum and R. Mersereau, "Fast Algorithms for the Multidimensional Discrete Fourier Transform," *IEEE Transactions on Acoustics, Speech, and Signal Processing*, 34(4):937-943, August 1986.
- [20] A. H. Karp, "Bit Reversal on Uniprocessors," *SIAM Review*, 38(1):1-26, 1996.
- [21] R. Nam'neh, K. A. Darabkh, and I. Jafar, "Efficient Bit Reversal Algorithms in Parallel Computers," *International Journal for Computers and Their Applications*, 19(3):154-165, September 2012.
- [22] S-C Pei and K-W Chang, "Efficient Bit and Digital Reversal Algorithm using Vector Calculation," *IEEE Transaction on Signal Processing*, 55(3):1173-1175, March 2007.
- [23] M. Portnoff, "An Efficient Parallel-Processing Method for Transposing Large Matrices in Place," *IEEE Transactions on Image Processing*, 8(9):1265-1275, September 1999.
- [24] J. Prado, "A New Fast Bit-Reversal Permutation algorithm based on a symmetry," *IEEE Signal Processing Letters*, 11(12):933-936, December 2004.
- [25] J. Rius and R. D. Porrata-Dorin, "New FFT Bit-Reversal Algorithm," *IEEE Transactions on Signal Processing*, 43(4):991-994, April 1995.
- [26] M. Rubio, P. Gómez , and K. Drouiche, "A New Superfast Bit Reversal Algorithm," *International Journal of Adaptive Control and Signal Processing* , 16:703-707, November 2002.
- [27] D. Scott, "Efficient All-to-All Communication Patterns in Hypercube and Mesh Topologies," *Proceedings of the 6<sup>th</sup> Distributed Memory Computing Conference*, pp. 398-403, Portland, Oregon, USA, May 1991.
- [28] R. C. Singleton, "An Algorithm for Computing the Mixed Radix Fast Fourier Transform," *IEEE Transactions on Audio and Electro Acoustics*, 17(2):93-103, June 1969.
- [29] J. Suh and V. Prasanna, "An Efficient Algorithm for Large-Scale Matrix Transposition," *Proceedings of the 2000 International Conference on Parallel Processing*, pp. 327-334, Toronto, Canada, August 2000.
- [30] D. Sundararajan, *The Discrete Fourier Transform: Theory, Algorithms and Applications*, World Scientific Publishing Company, Singapore, April 2001.
- [31] J. Walker, "A New Bit-Reversal Algorithm," *IEEE Transaction on Signal Processing*, 38(8):1472-1473, August 1989.
- [32] A. Yong, "A Better FFT Bit-Reversal Algorithm without Tables," *IEEE Transactions on Signal Processing*, 39(10):2365-2367, October 1991.
- [33] Z. Zhang and X. Zhang, "Fast Bit-Reversals on Uniprocessors and Shared-Memory Multiprocessors," *Journal of Scientific Computing*, 22(6):2113-2134, April 2001.



**Rami A. Al Na'mneh** is an Assistant Professor in the Department of Computer Engineering at Jordan University of Science and Technology. He received his bachelor degree in Computer Engineering from Jordan University of Science and Technology in 2000, the master and doctor of philosophy degrees from the University of Alabama in Huntsville in 2003 and 2006, respectively. His major research interests are in parallel programming, signal processing, and wireless communications.



**Khalid A. Darabkh** received his PhD degree in Computer Engineering from the University of Alabama in Huntsville, USA, in 2007 with honors. He is currently a Tenured Associate Professor in the Department of Computer Engineering at the University of Jordan, Amman, Jordan. He is engaged in research mainly on wireless sensor networks, queuing systems and networks, multimedia transmission, and steganography and watermarking. He authored and co-authored of at least seventy research articles and served as a reviewer in many scientific journals and international conferences. He serves on the Editorial Board of Telecommunication Systems, published by Springer, and Computer Applications in Engineering Education, published by John Wiley & Sons. Additionally, he serves as a TPC member of many reputable IEEE conferences such as GLOBECOM, LCN, VTC-Fall, PIMRC, ISWCS, and IAEAC. Moreover, he is a member of many professional and honorary societies, including Eta Kappa Nu, Tau Beta Pi, Phi Kappa Phi, and Sigma XI. He was selected for inclusion in the Who's Who Among Students n American Universities and Colleges and Marquis Who's Who in the World. As administrative experience at the University of Jordan, he served as Assistant Dean for Computer Affairs in the College of Engineering from Sept 2008 to Sept 2010. Additionally, he served as Acting Head of the Computer Engineering Department from June 2010 to Sept 2012.

# A Study of the Performance of Diversity Combining Schemes on Multipath Fading at 900MHz

A. J. Falade\*

University of Ilorin, Ilorin, NIGERIA

## Abstract

The work presents the investigation of Gaussian Minimum Shift Keying (GMSK) and Binary Phase Shift Keying (BPSK) transmission schemes with Department of Electrical and Electronics Engineering. E-mail: falade.alaba@yahoo.com. Phone: +2347053244999. both Maximum Ratio Combining (MRC) and Equal Gain Combining (EGC) diversity combining techniques over Rayleigh flat fading (RFF) channels in a digital mobile wireless system. The System model for the received signal was developed under L-propagation paths and then simulated. Randomly generated symbols and image data was used as the Information signal. The results obtained showed that BPSK had a higher error probability value than the corresponding GMSK scheme. The results also showed that due to GMSK high immunity to noise and other interfering signals, it provides a better performance than BPSK signalling scheme. MRC was observed to perform better in terms of mitigation of the interference induced by the Rayleigh channel than EGC diversity combining technique. The quality of the images received with both signalling schemes were in agreement with the Bit Error Rate (BER) results.

**Key Words:** Multipath fading, diversity combining, Rayleigh channel, bit error rate.

## 1 Introduction

The effectiveness of a communication system is a measure of the channel bandwidth and immunity to interference or noise. When a signal is transmitted over a radio channel in a digital mobile wireless communication system, it is subjected to multiple physical phenomena responsible for most of the characteristic features observed at the receiver end. Such phenomena include multipath fading and multiple access interference caused by co-channel users which are not orthogonal to the desired user [6]. Signal fading arises from multiple transmission paths with different phase shift and delay spread between the arrival of the first and last multipath signal seen by the receiver [3]. Various techniques can be employed for diversity combining but MRC and EGC are more effective [7, 10, 13]. In MRC, the signals are weighted according to their signal to noise ratio (SNR), and then the different signals are added together but only after being co-

phased (that is, the different signals are delayed to ensure that they all have the same phase for constructive addition). The main drawback of using MRC is that the signal level and noise power at each branch needs to be correctly estimated for all instances in time. EGC is similar to the MRC except that the weighting is set to 1 for all signals. The Rayleigh distribution is commonly used to describe the statistical time varying nature of the received envelope of a flat fading, or the envelope of an individual multipath component. In the RFF channel model, it is assumed that the channel induces amplitude, which varies according to the Rayleigh distribution.

The structure and the contribution of this paper are organized as follows. In Section 2, a related work is given. Sections 3 and 4 cover the system model and diversity combining models, respectively. Section 5 is based on the simulation results and discussion. Section 6 concludes the paper.

## 2 Related Work

M. Kahn derived the combining weights of the optimal linear combiner for dual diversity [8]. His techniques were used to generate results of higher order diversity scheme known as MRC. A combining technique to mitigate the effects of intersymbol interference (ISI) was later introduced by [5]. Studies of various diversity combining techniques have been carried out in [12]. Adachi [2] gave a detailed BER performance of 16 star-quadrature amplitude modulation (STAR-QAM) in the Rayleigh fading channel. Average bit error rate expressions for BPSK and binary frequency shift keying (BFSK) were analysed as infinite series in [1]. Alamouti [4] employed a simple transmit diversity technique for mitigating multipath. A comprehensive study of a joint multipath Doppler diversity in mobile wireless Communications was carried out by [11].

Most of the past works were excellent particularly on the subject of fading channels and diversity reception, with many cases having been thoroughly analysed; but none of the papers have simultaneously presented simulation and experiment by the application of image data acquisition using MRC and EGC diversity technique. Hence, the study of GMSK and BPSK transmission schemes with both MRC and EGC diversity combining techniques over RFF channels in a digital mobile wireless environment is presented in this work. The channel is assumed to be frequency non-selective flat fading. Random data were generated and modulated with each of the modulation schemes. The result is filtered using Gaussian low

---

\* Department of Electrical and Electronics Engineering. E-mail: falade.alaba@yahoo.com. Phone: +2347053244999.

pass for GMSK to reduce the spectral spreading of the sidebands. Also, a rectangular pulse shaping filter is employed to reduce ISI induced in the system for BPSK to achieve suitable transmission through the wireless mobile channel. The bit error rate is the measure used in the performance evaluation.

### 3 System Model

A single mobile to base station communication with one antenna over a frequency non-selective channel was considered first and other interfering signals are added together and modelled as an additive white Gaussian noise. The received signal by the base station through only one path is given by [3] as:

$$r(t) = h(t, T)S(t) + n(t) \quad (1)$$

where  $h(t, T)$  is the time varying impulse response of the channel,  $S(t) = S_{GB}(t)$  is the transmitted GMSK and BPSK signal and  $n(t)$  is interfering signals modelled as additive white Gaussian noise (AWGN). For GMSK scheme, the signal is represented by

$$m(t) = \sin(2\pi f_c t)I(t) + \cos(2\pi f_c t)Q(t) \quad (2)$$

where  $f_c$  is the carrier frequency,  $I(t)$  is the inphase baseband signal and  $Q(t)$  is the quadrature baseband signal. The inphase and quadrature baseband signals are the cosine and sine of the output of the integrator from Gaussian low pass filter (GLPF).

### 4 Diversity Combining Model

#### 4.1 Maximum Ratio Combining (MRC)

The output of MRC is a weighted sum of all branches. According to Alamouti [4], the channel at time  $t$  may be modelled by complex multiplicative distortion

$$h(t, T) = \alpha_i(t, T) \exp(j\theta_i(t, T))\sigma(T - T_i(t)) \quad (3)$$

where  $\alpha_i(t, T)$  is the amplitude of  $i^{\text{th}}$  multipath at  $t$  and  $T$ , and  $\sigma$  is the impulse function that determines the specific multipath component at time  $t$  and delay  $T$ .

With two independent identically distributed paths, the transmitting medium between the first transmit antenna and receiver (path 1) is denoted by  $h_0$ , while  $h_1$  denotes the medium between the second transmit antenna and receiver (path 2) at a given time. The output baseband signals for the first and second receiver through paths 1 and 2 are

$$r_0(t) = h_0(t, T)s_0(t) + n_0(t)$$

and

$$r_1(t) = h_1(t, T)s_1(t) + n_1(t)$$

respectively, the resultant received signal is

$$S_{G,B}(t) = h_0^*(t, T)r_0(t) + h_1^*(t, T)r_1(t) \quad (4)$$

where  $h_0^*(t, T)$  and  $h_1^*(t, T)$  are the complex conjugate of the channel impulse responses of path 1 and 2, respectively. The complex conjugate of the channel impulse response cancels the phase variations that the channel introduced. By substituting the values of  $r_0(t)$  and  $r_1(t)$  into Equation (4), we obtain

$$\begin{aligned} S_{G,B}(t) &= h_0^*(t, T) * [h_0(t, T)s_0(t) + n_0(t)] \\ &+ h_1^*(t, T) * [h_1(t, T)s_1(t) + n_1(t)] \end{aligned} \quad (5)$$

This is the output of the MRC, where  $s_0$  and  $s_1$  are the received signals at time,  $t$  and  $t+T$ , and  $n_0$  and  $n_1$  are the complex noise and interference. Combining the Equations (3), (4) and (5) together, we get

$$S_{G,B}(t) = [\alpha_0^2(t, T) + \alpha_1(t, T)^2]s_0 + h_0^* * n_0 + h_1^* * n_1 \quad (6)$$

#### 4.2 Equal Gain Combining (EGC)

In an EGC receiver, like the case of MRC, both branch signals are multiplied by the same branch gain ( $G$ ) and the resulting signals are co-phased and summed. The resultant output signal is connected to the demodulator, therefore, Equation (4) can be re-written as

$$S_{G,B}(t) = G_0(t, T)r_0(t) + G_1(t, T)r_1(t) \quad (7)$$

where  $G_0(t, T)$  and  $G_1(t, T)$  are the gain of each path 1 and 2, respectively. Assuming that the equal path gain is represented by  $G(t, T)$ .

$$\begin{aligned} S_{G,B}(t) &= G(t, T) * [h_0(t, T)s_0(t) + n_0(t)] \\ &+ G(t, T)[h_1(t, T)s_1(t) + n_1(t)] \end{aligned} \quad (8)$$

This is the output of the EGC.

### 4.3 Multipath Channel Parameters

To compare the performance of the BPSK with the GMSK signalling schemes, the system model simulation is given in Figure 1 for (i) BPSK/GMSK with 2-path MRC, and (ii) BPSK/ GMSK with 2-path EGC, where  $h_1$  and  $h_2$  in (i) are replaced with input and output gains.

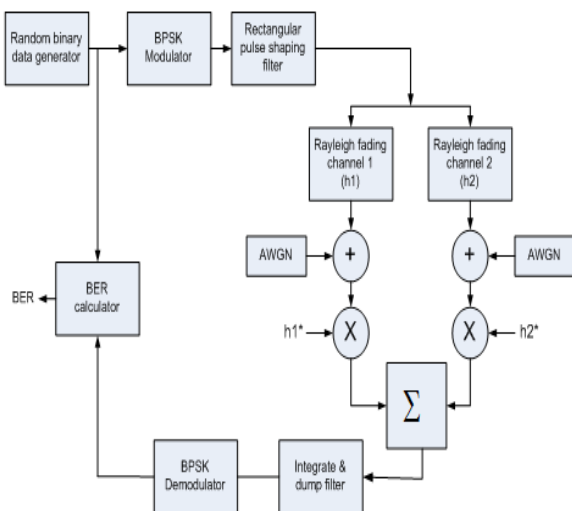


Figure 1: Simulation model for case (i) MRC with BPSK/GMSK as shown, and case (ii) EGC with BPSK/GMSK signalling schemes, where  $h_1$  and  $h_2$  in case (i) are replaced with input and output gains

### 4.4 Simulation Implementation

The BER performances of MRC and EGC diversity techniques using BPSK and GMSK modulation schemes were obtained by numerical simulation of the system algorithm. The development of the data needed for the performance evaluations are as follows: (a) defining the systems' parameters, (b) determining the constraints and conditions needed for the simulation, (c) writing the pseudo-code or algorithm, (d) writing the codes in steps, and (e) debugging the code and making modifications in steps and testing. The signals processing toolboxes of MATLAB were used to simulate, generate and transmit random data and image data, and in the plotting of the graphs.

The signal strength in mobile radio at the receiver end changes from time to time due to multipath effects. The received signal becomes flat fading if the radio channel is characterized with linear phase response and constant gain with a bandwidth larger than the bandwidth of the transmitted signal. To obtain the spectral characteristics of the transmitted signal at the receiver, both BPSK and GMSK modulation schemes are explored separately at the transmitter. The channel is subjected to thermal noise, represented by AWGN, caused by fluctuations in the gain of the channel. Using non-line of sight, multiple reflected rays representing multipath Rayleigh fading are formed. MRC and EGC techniques are

then employed at the receiver to mitigate the effects of the multipath on the received signals.

### 4.5 Data Acquisition

Data sources for the simulation are those generated randomly and the image data of University of Ilorin Senate Building (UISB). An enhanced modulation technique designed to increase network capacity and data rate in GSM networks can provide data rates up to 384 kbps in third generation (3G). Random data of 100,000 bits were used to determine the actual error bits when subjected to multipath fading while image signal complements the output of the results. The parameters and system configuration used in the simulation were chosen from the standard of the mobile systems [9], as summarized in Table 1. An assumption of a mobile speed of 30km/h were made for the receiver (mobile antenna), which introduces the fading effects (Doppler shift) relative to the base station. Doppler spread was computed to be 25Hz and the coherence time is  $4 \times 10^{-2}$  sec. The multipath delay spread of  $2.0 \times 10^{-7}$  sec gives 5MHz. This is larger than the assumed bandwidth of 200Hz, indicating frequency non-selective/flat fading channel.

Table 1: Simulation parameters and configuration [9].

Parameter	Value
Number of bits transmitted	100,000 bits
Carrier frequency, $f_c$	900 MHz
Bit rate, $R_b$	2.4 kb/s
Mobile speed	30 km/h
Bandwidth of signal	200 kHz
Normalized bandwidth of Gaussian filter, BT	0.3
Gaussian filter taps	21
Image type / dimension	JPEG / 90x60 pixels
Multipath delay spread	$200 \times 10^{-9}$ sec
Noise	AWGN
Number of paths, L	2, 3 and 4

## 5 Results and Discussion

The results obtained from the simulation of both random data and UISB image data over a non-selective RFF channel for GMSK and BPSK signalling schemes using both MRC and EGC at the receiver are shown in Figures 2 to 14. Figure 2 is the BER of BPSK and GMSK modulation schemes over RFF and AWGN channels. Figures 3 and 4, represent a comparison of EGC and MRC for 2 paths with BPSK and GMSK signalling, respectively. From the graph of Figure 3, the two diversity combining techniques have the same BER performance for SNR between 0-2dB. As the SNR increases beyond 2dB, 2-path MRC is observed to provide a better performance than 2-path EGC diversity technique in terms of fading mitigation. Similarly, Figure 4 gives the comparison of EGC and MRC for 2-paths using GMSK modulation scheme.

The graph shows that 2-path MRC and EGC have the same error probability for SNR of 0-2dB. Beyond SNR of 2dB, the 2-path of MRC is observed to have a lower BER than EGC. This implies a better performance of 2-path MRC over 2-path EGC. Figures 5 and 6 are the BER performance of BPSK

signalling scheme for both MRC and EGC, respectively. The varying paths are assumed to be independent identically distributed. Figures 7 and 8 show the profile of BER performance of GMSK signalling scheme with MRC and EGC at the receivers over a Rayleigh channel, respectively.

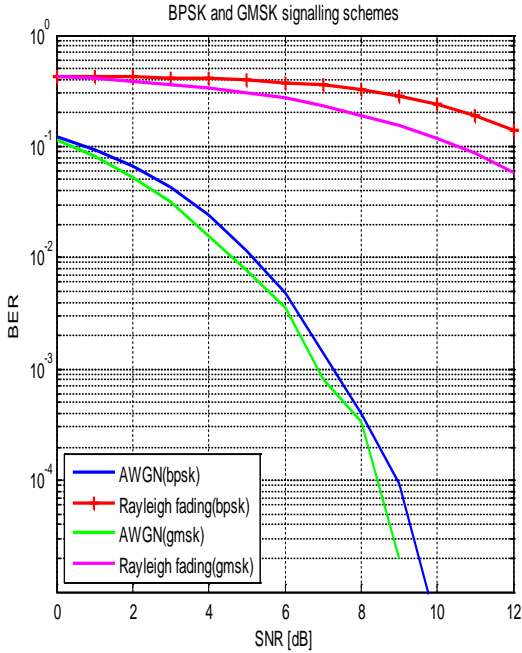


Figure 2: BER of BPSK and GMSK modulation schemes over flat Rayleigh fading channel and AWGN channel

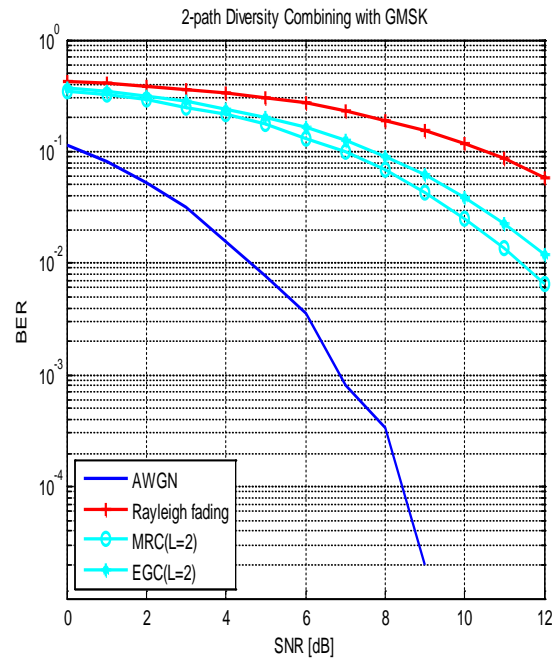


Figure 4: Comparison of EGC and MRC for 2 paths using GMSK modulation scheme

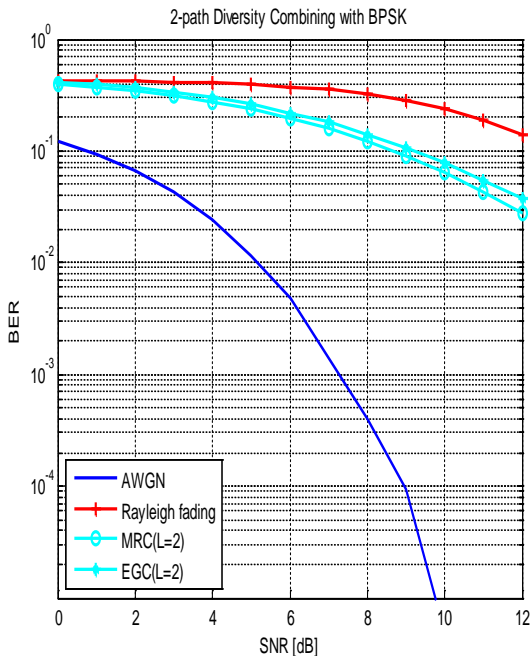


Figure 3: Comparison of EGC and MRC for 2 paths using BPSK modulation scheme

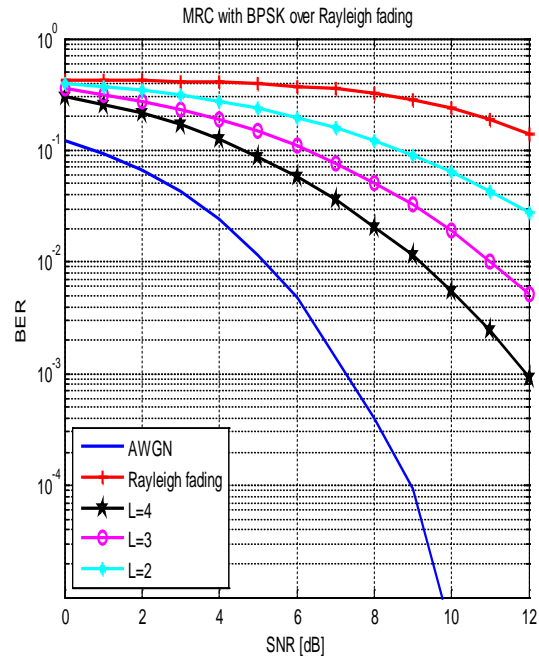


Figure 5: BER comparison for varying paths of MRC using BPSK modulation scheme over Rayleigh channel

For a total of 100,000 bits of GMSK signals transmitted at SNR of 6dB in Rayleigh flat fading channel, 26,930 bits were changed by the channel indicating number of bit errors. But with the introduction of 2-paths, 3-paths and 4-paths MRC at the receiver, the high erroneous bits were reduced to 13,260 bits, 7,570 bits, and 4,320 bits, respectively. Also, with 2-path, 3-paths, and 4-paths EGC at the receiver, the high erroneous bits are also reduced to 16,560 bits, 9870 bits, and 6,340 bits, respectively. The original high erroneous bits were due to the effects of delay and Doppler spread without diversity combiner. The later reduction in bit errors resulted from varying paths in MRC and EGC diversity combiner separately employed at the receiver.

In the same vein, the image transmitted through AWGN channel produced a close result compared with the original transmitted signal. When subjected to a Rayleigh fading channel at SNR of 12dB, there was a great distortion in the original message as shown in Figure 9.

Figures 10 and 11 show the application of diversity combining techniques to image data at SNR of 12dB and 6dB respectively, using BPSK for comparison. When 2-path of MRC/EGC is introduced at the receiver, a better image output than in a flat Rayleigh fading channel is obtained. When 3 path and 4-path MRC/EGC is employed respectively, a better image at the output in order of higher paths is produced. The image quality output is improved for each of the two diversity combiner but MRC provided a better image than EGC. Figure 12 shows the application of diversity combining techniques to image data at SNR of 12 dB using GMSK. An image was transmitted through an AWGN channel which produced a close result to the original transmitted signal, but when subjected to a Rayleigh fading channel at SNR of 12dB, there

was a great distortion in the original message. When 2-path MRC/EGC is employed at the receiver, a better image output than in a flat Rayleigh fading channel is produced. The employment of 3-path MRC/EGC provides a better result than a 2-path MRC/EGC diversity. The 4-path MRC/EGC has the best image for GMSK and BPSK as shown in Figures 13 and 14 for 12dB and 6dB, respectively for comparison.

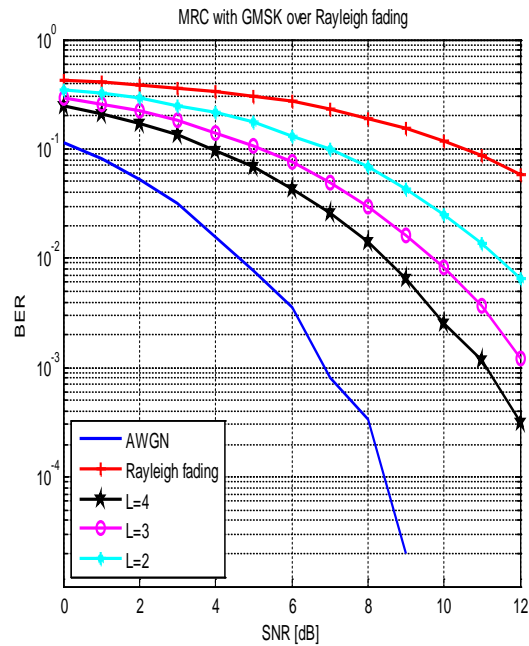


Figure 7: BER comparison for varying paths of MRC using GMSK modulation scheme.

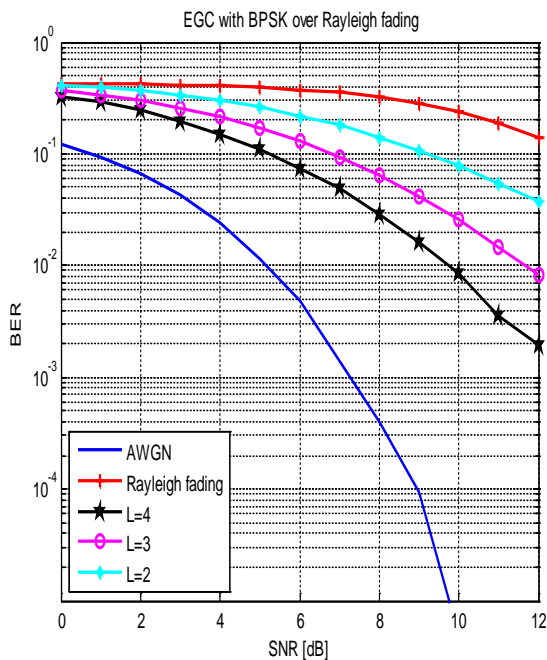


Figure 6: BER comparison for varying paths of EGC using BPSK modulation scheme over Rayleigh channel

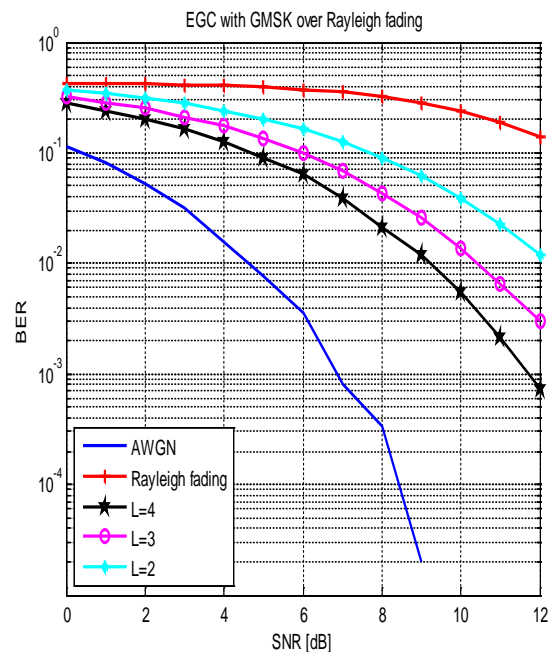


Figure 8: BER comparison for varying paths of EGC using GMSK modulation scheme

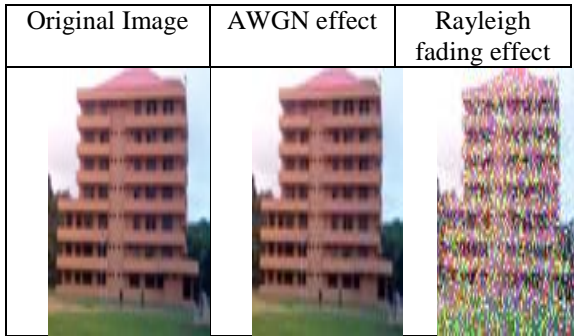


Figure 9: Image data through AWGN channel and the corresponding Rayleigh fading effect at SNR of 12dB using BPSK

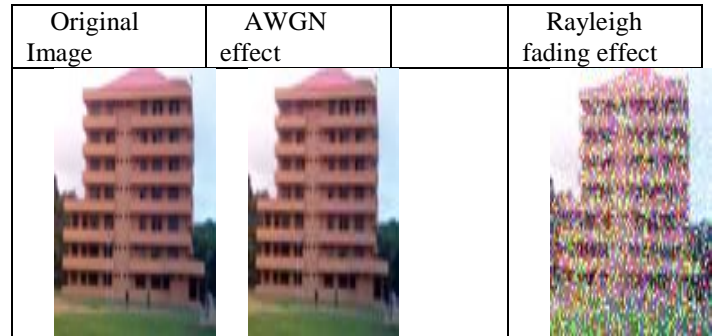


Figure 12: Image data through AWGN channel and the corresponding Rayleigh fading effect at SNR of 12dB using GSMK

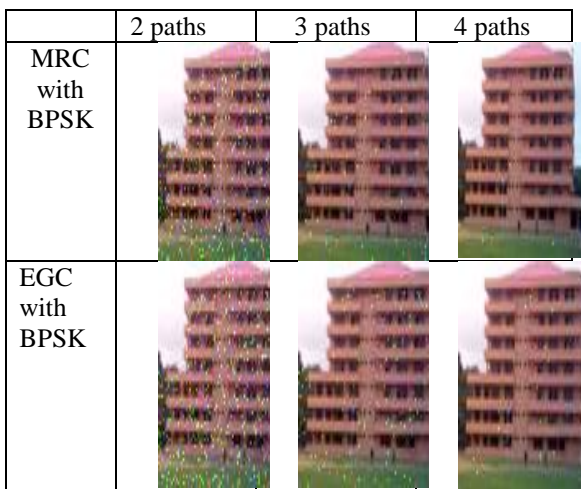


Figure 10: Application of diversity combining techniques to image data at SNR of 12dB using BPSK

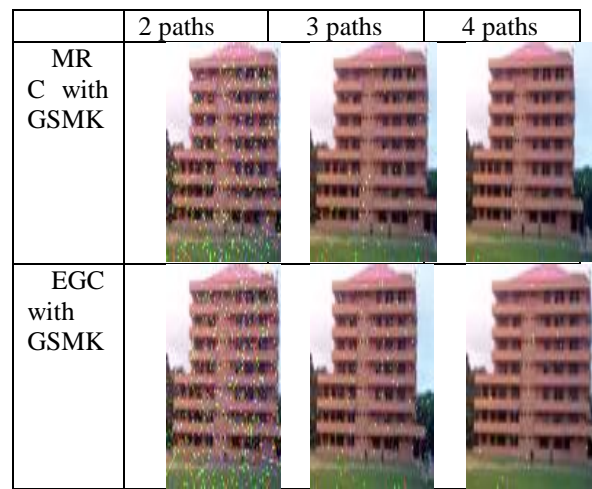


Figure 13: Application of diversity combining techniques to image data at SNR of 12 dB using GSMK

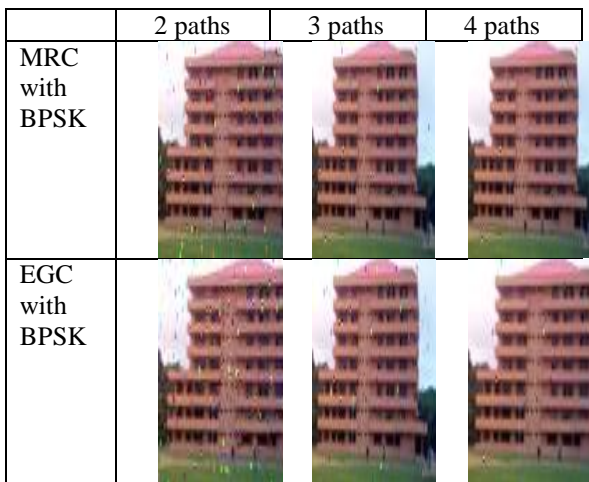


Figure 11: Application of diversity combining techniques to image data at SNR of 6 dB using BPSK

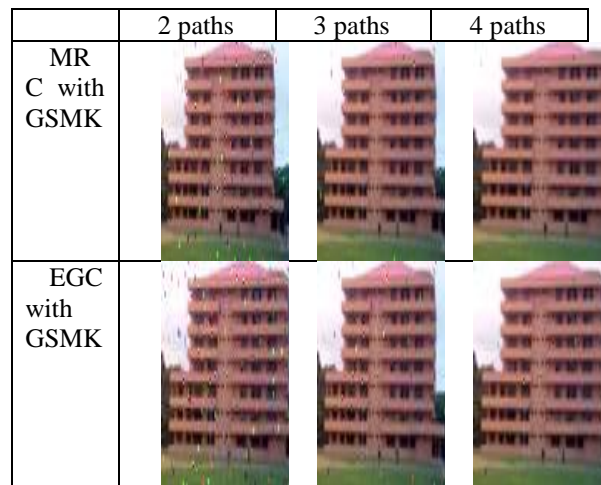


Figure 14: Application of diversity combining techniques to image data at SNR of 6 dB using GSMK

The image outputs further support the results from the profiles obtained in Figures 2 to 8, when comparing MRC and EGC. For the same L-path diversity, though both EGC and MRC provide an improvement in the output, but MRC has a better image than EGC.

## 6 Conclusions

The system model for the received signal at a mobile speed of 30km/hr [9] has been developed and simulated. The BER for the system was evaluated for each of the varying paths of MRC and EGC diversity combiner. It was found that the performance depends on the number of diversity in each branch. BPSK signalling schemes with both diversity combiner techniques separately employed at the receiver with MRC presented a clearer image than EGC diversity combiner. The simulation results showed that GMSK signalling scheme performed better than BPSK signalling when both were subjected to the same non-selective RFF channel, due to lower error bits received when transmitting the same number of bits. This showed that GMSK is more immune to noise than the BPSK. In GMSK signalling schemes for image transmission with EGC and MRC combiner at the receiver, the results obtained show that both diversity combiner techniques mitigated the effect of fading but GMSK signalling has a better performance in terms of a lower BER than BPSK signalling scheme. This is evident from the UISB image modulated by these signalling schemes. Therefore, the results showed that GMSK signalling scheme is better than BPSK when employing MRC diversity combining technique at the receiver with a Rayleigh frequency non-selective fading channel. This confirmed that GMSK signalling scheme perform better than BPSK signalling scheme due to lower error bits received when transmitting the same number of bits.

In GMSK signalling scheme for image transmission with EGC and MRC combiner at the receiver, the results showed that both diversity combiner techniques mitigated the effect of fading, but MRC presented a better image at the output than EGC diversity combining. Hence, by comparing the performance of GMSK with BPSK signalling for image transmission using both MRC and EGC at the receiver, it was observed that GMSK signalling has better overall performance in terms of low BER than BPSK signalling scheme. This is evident from the UISB image modulated by these signalling schemes. This concludes that GMSK signalling scheme is better than BPSK when employing MRC/EGC diversity combining technique. These signalling schemes take place at the receiver with a Rayleigh frequency non-selective fading channel.

## References

[1] V. A. Aalo, T. Piboongunon, and I. Cyril-Daniel, "Bit Error Rate of Binary Digital Modulation Schemes in Generalized Gamma Fading Channels," *IEEE Comm. Letters*, 9:139-141, 2005.

- [2] F. Adachi and M. Sawahashi, "Performance Analysis of Various 16 Level Modulation Schemes under Rayleigh Fading," *Electronic Lett.*, 28:1579-1581, 1992.
- [3] Z. K. Adeyemo and R. O. Abolade, "Comparative Analysis of GMSK and BPSK Signalling Scheme with MRC over a Rayleigh Fading Environment," *Adv Materials Res.*, 367:205-214, 2012.
- [4] S. M. Alamouti, "A Simple Transmit Diversity Technique for Wireless Communications," *IEEE J. on Selected Areas in Comm.*, 16(8):1451-1458, 1998.
- [5] M. V. Clark, L. J. Greenstein, W. K. Kennedy, and M. Shafi, "MMSE Diversity Combining for Wideband Digital Cellular Radio," *IEEE Trans. on Comm.*, 40:1128-1135, 1992.
- [6] B. P. Constantinou and H. A. Howard, "Linear Time Multiuser Detector using Antenna Array Processing for Wireless CDMA Capacity Improvement," *IEEE J. on Selected Areas in Comm.*, 19(2):254-265, 2001.
- [7] A. J. Coulson, A. G. Williamson, and R. G. Vaughan, "Improved Fading Distribution for Mobile Radio," *IEE Proc. F-Communication*, 145:197-200, 1998.
- [8] L. Kahn, "Ratio Squarer," *Proceedings of IRE*, 42:1704, 1954.
- [9] Recommendation ITU-R F.1487. Testing of Modems with Bandwidths of up to about 12kHz using Ionospheric Channel Simulators. 2010; Accessed 6 December 2013. Available: <https://www.itu.int/rec/R-REC-F.1487-0-2000005-1/en>.
- [10] V. K. Sakarello, D. Skraparlis, A. D. Panagopoulos, and J. D. Kanellopoulos, "Cooperative Diversity Performance of Selection Relaying over Correlated Shadowing," *Physical Communication*, 4(3):182-189, 2011.
- [11] A. M. Sayeed and B. Aazhang, "Joint Multipath Doppler Diversity in Mobile Wireless Communications," *IEEE Transactions on Communications*, 47(1):123-132, 1999.
- [12] M. Schwartz, W. R. Bennett, and S. Stein, *Communication Systems and Techniques*, McGraw-Hill, New York, 1966.
- [13] R. You, H. Li, and Y. Bar-Ness, "Diversity Combining with Channel Estimation," *IEEE Trans. Commun.*, 53(10):1655-1662, 2005.



**Alaba John Falade** received the B. Sc. degree in Engineering Physics in 1988, M. Eng. Degree in Electrical and Electronics Engineering from University of Benin, Benin-City in 1995, and a Ph.D. with an area of specialization in Telecommunication from University of Ibadan, Nigeria in 2005. He is a Senior Research Fellow in the Department of Electrical and Electronics Engineering. His current research interests include radio propagation and wireless communication. He is a member of Nigerian Society of Engineers and IEEE.

# A Personal Identification System Based on Iris Recognition

Khalid A. Buragga\*

Northern Border University, Saudi Arabia.

Sultan Aljhdali<sup>†</sup> and Ahmad. M. Sarhan<sup>†</sup>

Taif University, Saudi Arabia

Marcel Karam<sup>‡</sup>

American University of Beirut, Beirut, Lebanon

## Abstract

In this paper, a biometric personal identification system based on iris recognition is proposed and presented. The developed system first isolates the iris from the rest of the input image. The separated iris is then normalized and transformed using Wavelets. Classification features are extracted using a novel thresholding technique that keeps track of the relative amplitudes and locations of the extracted high-energy coefficients. An Artificial Neural Network (ANN) is then employed on the extracted features to classify the input image. To show the validity and merits of the proposed system, its performance is compared to that of vector quantization (VQ), a minimum-distance classifier that uses the Euclidean distance. Simulation results show that the proposed ANN system produces a low recognition error of less than 5% and always outperforms the VQ system. The iris images used in this study are obtained from the CASIA database,

**Key Words:** Iris, wavelets, artificial neural network (ANN), vector quantization (VQ), biometrics, feature extraction.

## 1 Introduction

In many biometric applications such as access control, information protection, and authentication, it is important to determine the identity of a person. Conventional methods of recognizing the identity of a person by using identification cards or passwords are not always reliable since passwords can be forgotten; and identification cards can also be lost, stolen, or forgotten. Consequently, there is tremendous interest in identification (authentication) methods which depend on measures that cannot be lost, forgotten, or stolen. Biometric methods identify people based on physiological characteristics such as face, fingerprint, palm print, hand geometry, DNA, iris, and retina. Behavioral characteristics such as gait, voice, and handwriting (signature) can also be used by biometric

systems. In general, any human behavioral or physiological characteristic could be a biometric given that it satisfies the following requirements: (a) stability (the characteristic should be invariant with time), (b) uniqueness (no two persons are the same with respect to the characteristic), (c) universality (every person has the characteristic), and (d) collectability (the characteristic can be measured quantitatively) [3, 15].

Among all the human physical characteristics, the iris has been widely regarded as the most accurate biometric. The iris has many outstanding properties including its unique visible characteristics, stability over a person's lifetime, and its secure nature (being an internal organ, it is difficult to replace or remove the iris; thus, decreasing the possibility of deceiving the recognition system). The iris is the colored ring (membrane) of the eye, bounded by the white sclera and the black pupil. It controls the amount of light reaching the interior of the eye (retina). The iris and the pupil are covered by a clear covering called the cornea. The iris consists of pigmented fibro vascular tissue known as stoma. It is the most forward portion of the eye and the only one seen on trivial inspection. The iris has an intricate structure that includes a rich pattern of minute characteristics such as coronas, furrows, freckles, and crypts.

In this study, we propose and develop a biometric system for iris recognition. The system employs an integro-differential operator to locate the iris structure. Distinctive features are then obtained from the segmented iris image using an operation based on Wavelet packet decomposition (WPD) and a thresholding technique that keeps the values and the locations of the high-magnitude approximation coefficients while discarding the rest of the approximation and detail coefficients. Classification of the iris feature vector is then achieved using an ANN classifier. To prove the validity and robustness of the proposed method, its performance is compared to that of a vector quantization (VQ) system that uses the Euclidean distance. To test the proposed system, we use the Chinese academy of sciences institute of automation (CASIA) database [2], a freely available iris database containing images of human irises.

## 2 The State of the Art in Iris Recognition

This survey provides a brief coverage of the current state of

\* Computer Science Department, College of Computing and IT. E-mail: nbu10@nbu.edu.sa.

<sup>†</sup> Dept. of Computer Science. E-mail: aljhdali@tu.edu.sa, and a.sarham@tu.edu.sa

<sup>‡</sup> Department of Computer Science. E-mail: mk62@aub.edu.lb.

the art in iris biometrics and its commercial applications. Most of the research publications in this field have made contributions to one of the four main areas in iris biometrics: image acquisition, iris segmentation, feature extraction, and classification. The most important contribution in the early history of iris biometrics was made by Daugman [4, 5], where he described an automatic iris recognition system. Daugman's approach has laid the ground for most of the later research in iris biometrics and has become a standard reference model. In [6] Daugman describes a border-control application of iris recognition that is currently being used in the United Arab Emirates (UAE) to check visitors to the country. The UAE database contains 632,500 different iris images. Daugman reports that by using an iris recognition system, about 47,000 people have been caught trying to enter the UAE using false travel documents. The UAE police reports that so far all the matches have also been confirmed by other means. Another commercial example of the successful use of iris identification systems is presented by the Cairo-Amman Bank (CAB) in Jordan. In 2008, the CAB, in cooperation with the leading biometric security manufacturer Iris Guard, was the first bank in the world to implement the ocular security scan technology. The CAB now offers this service in more than 80 branches and 215 ATM machines [1].

Kekre et al. worked on the iris recognition problem using Haar Wavelets for feature extraction and the Euclidean distance for classification [13]. They used the Palacky database and found that Haarlets level-5 outperforms lower-level Haarlets. Sarhan used the CASIA database and developed an iris recognition system in which he used an ANN for classification and the discrete cosine transform (DCT) for feature extraction [22]. The successful method implemented by Sarhan did not involve segmentation and the DCT was applied to the whole image rather than dividing the image into blocks as performed in JPEG compression. Sarhan also tackled the iris feature extraction problem using Wavelets [28]. A comparison of different iris feature extraction methods was developed by Vatsa et al. [32]. An experimental comparison of different segmentation methods was developed by Proenca et al. [20]. Proenca also developed an iris recognition system using structural pattern analysis methods [18]. Phillips et al. presented on the ICE web site an evaluation report of the current state-of-the art in iris biometrics [17]. For the purpose of reducing the transmission time of iris images, Ives et al. worked on the compression of iris images in portable iris systems such as in law enforcement applications [12].

Several iris databases are freely available online. The list includes the CASIA database, the iris Challenge Evaluation (ICE) database [14], the IIT Delhi (IITD) iris database [11], and the UBIRIS database, which was developed by the University of Beira Interior in Portugal [19]. The UBIRIS v.1 database contains 1877 images collected from 241 eyes and has a spatial resolution of  $800 \times 600$  pixels. It simulates less constrained imaging conditions. As an alternative to iris database collection, Wei et al. presented a framework to synthesize large realistic iris databases [33]. Segmented iris images are available from the Palacky database, a relatively

small iris database created at Palacky University [16]. It contains  $3 \times 128$  segmented iris images ( $3 \times 64$  left eyes and  $3 \times 64$  right eyes). The images have a RGB format with spatial resolution of  $576 \times 768$  pixels and 24 bits per pixel. Figure 1 shows three iris images of a left eye.

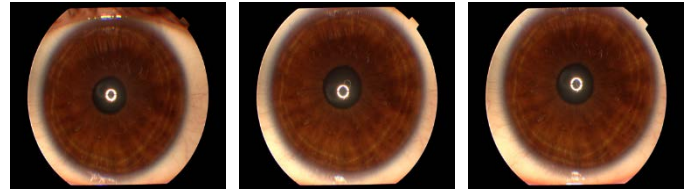


Figure 1: Palacky database: Three iris images of the same eye [16]

### 3 Material and Methods

#### 3.1 System Block Diagram

A block diagram of the proposed system is depicted in Figure 2. The input of the system is an image of the iris. The iris database used in this paper is the CASIA, v.2 database which contains 1200 raw eye images. The images are for 30 persons. For each person, there are 20 iris images for the left eye and another 20 images for the right eye, giving a total of 40 images for each person. Note that the left and right irises for a given person are different from each other. The original size of each image is  $480 \times 640$  pixels, with 256 grey levels per pixel. We used images from seven classes (right eyes only), with 20 samples per class. Thus, our dataset contained 140 images; half of which were used for training and the other half were used for testing.

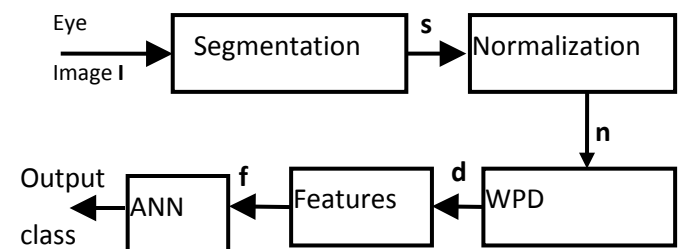


Figure 2: Block diagram of the proposed system, where **s**, **n**, **d**, and **f** represent the segmented iris vector, normalized iris vector, and the feature vector, respectively

#### 3.2 Iris Segmentation

Many types of image segmentation techniques have been used in the literature. The list includes histogram-based, graph cuts, and region-based techniques. The histogram techniques are mainly used to tackle the threshold problem in histogram- and region-based methods. The histogram technique produces a binary image based on the threshold value. The intensities of object and background pixels tend to cluster into two sets in

the histogram with the threshold between these two sets. In general, it is difficult to find a universal threshold for all cases to determine the threshold value for segmentation. Consequently, graph cut image segmentation techniques used two kinds of seed pixel as “object” and “background” to provide hard constraints for segmentation.

The region-based segmentation technique segments an image which has strong boundaries into several small regions, followed by a merging procedure that employs a specific threshold. In both histogram-based and region-based segmentation techniques, if the threshold is not accurate, the contour of the object will be destructed. Wu et al. described a top down region-based image segmentation technique for medical images that contain three major regions: background and two tissues. This method is mainly used to segment 2D images and cannot be applied to segment 3D images.

Commonly used iris segmentation methods include the integro-differential, active contour models, and the Hough transform techniques. The classical Hough transform was originally introduced by Paul Hough as an image feature extraction technique for identifying lines in the image [8]. Later, the generalized Hough transform technique was presented by Richard Duda and Peter Hart in 1972 to identify positions of arbitrary shapes, especially circles and ellipses [7]. The Integro-differential operator introduced by Daugman can be used as a circular edge detector algorithm that assumes circular structure of the pupil and limbus. It finds all circles in an image. The sum of pixel values within each circle is compared to the values of adjacent circles. The circle with the maximum difference from its adjacent circles is recognized as the iris.

Iris discs have different sizes for different input images. However, for proper processing, the input irises must have the same size. Here we propose an operation that unifies the sizes of all the irises in the dataset. Specifically, the input iris disc is normalized by converting it to a vector whose length is the same as the length of the vector corresponding to the smallest iris disc in the dataset. In the next stage of the proposed system, the normalized vector is transformed using the WPD.

### 3.3 Wavelet Packet Decomposition

Lossless transforms do not change the information content or energy of the signal. Suitably selected transforms can be used effectively in various signal and image processing applications including compression, restoration, coding, and feature extraction. A new transform, known as the wavelet transform (WT), has proven to be more effective in many DSP applications and has been used widely in recent years. The most commonly used wavelets are the Daubechies (db) and the Haar wavelets. The proposed system employs the Daubechies db1 wavelet which is considered the first and simplest wavelet.

In wavelet nomenclature, approximations and details are often used where details are the high-frequency, low-scale components, and approximations are the low-frequency, high-scale components of the signal. The discrete Wavelet transform (DWT) is a subset of the wavelet packet

decomposition (WPD) transform.

Because of its outstanding energy concentration capability, the DWT has found many practical applications in signal and image compression. The powerful energy compactness property of the WPD is evident in the limited number of high-magnitude coefficients found in the transformed signal. The strong energy compactness of the WPD makes it very useful in pattern recognition applications [25, 27]. In the proposed system, we exploit the signal compression characteristic of the WPD to form a valid feature vector ( $f$ ) representing the input iris vector. Since the most important part of a signal is often contained in the lower-frequency components of the signal spectrum (approximation coefficients), we propose a scanning technique that keeps the values and locations of the high-magnitude approximation coefficients while discarding the rest of the approximation coefficients. The details coefficients are not considered here since they represent a small fraction of the signal energy. As illustrated by Figure 3, the proposed masking technique keeps only the higher-magnitude coefficients (positive and negative) and also preserves their locations. Note that Figure 3 uses a threshold level of 15.1; thus, the scanning operation keeps only the coefficients whose absolute values are greater than 15.1.

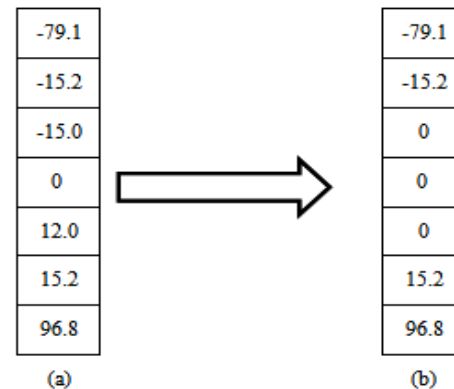


Figure 3: Illustration of the proposed masking operation using a threshold level of 15.1: (a) Input approximation coefficients and (b) output feature vector

The output of the masking operation performed on the approximation vector  $d$  produces the feature vector  $f$ . In the last stage of the proposed system,  $f$  is presented to an ANN for classification. ANNs are trainable algorithms that can “learn” to solve complex problems from training data that consists of pairs of inputs and targets (desired outputs). ANNs have been successfully used in many applications including prediction, classification, image processing, regression, and adaptive control [21, 23, 29-30].

The basic building block of the ANN is the neuron, depicted in Figure 4. The output of the neuron is a linear combination of its inputs. The neuron’s scaled output  $y$  is given by  $y = f(a)$ , where  $f$  is a transfer function. A typical ANN consists of interconnected neurons. The weights of the neurons are calculated iteratively so as to optimize a certain criterion such

as the Mean-Squared-Error (MSE) between the ANN output and its desired output. Optimum weights in the sense of Least Squared Errors were derived by Widrow and Hoff and the algorithm is known as the Widrow-Hoff rule or as the Least Mean Squares (LMS) algorithm.

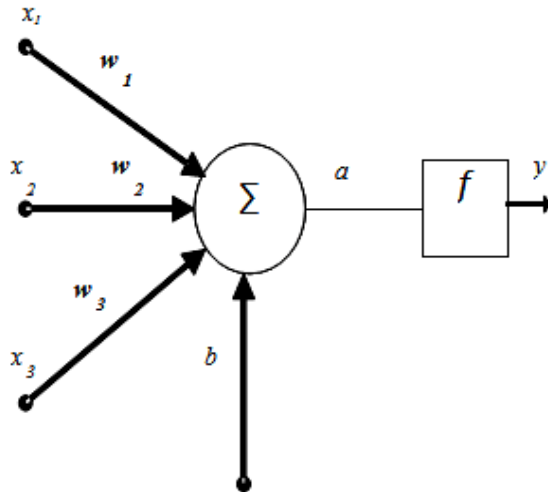


Figure 4: The structure of a single neuron:  $x_i$ ,  $w_i$ ,  $b$ , and  $a$  are the inputs, weights, bias, and output, respectively

All the ANNs examined in this study are trained with the same sets of inputs and outputs that are used to train the VQ system, and have the following specifications:

1. The networks receive as input the feature vector representing the input iris sample.
2. The network structure is a two-layer feed-forward neural network. The output layer has seven neurons in order to represent seven classes. For example,
3.  $y = [0 \ 0 \ 1 \ 0 \ 0 \ 0 \ 0]^T$ , where T denotes the transpose operation, represents the third class.
4. The learning algorithm used here is the back propagation algorithm.
5. The log sigmoid function, which can approximate binary values, is used as the transfer function of the output layer.

To prove the merits of the proposed system, its performance is compared to that of a VQ system that uses the Euclidean distance. For decades, VQ has been used as a popular technique in applications involving signal and image compression. In recent years, VQ has been effectively used as a classifier in pattern recognition applications [24, 26].

An M-level vector quantizer is a mapping of each input vector to a specific partition defined by an index and an associated vector called a code word or a reproduction vector (class). The collection of M code words is referred to as the code book. The VQ technique uses a minimum-distance rule to classify(encode) a test or input vector (whose class is unknown). Several distortion measures have been proposed in the literature including the Euclidean distance, the Manhattan distance, the Holder norm, the Hausdorff distance, the

Hamming Distance, the Mahalanobis distance, the Chebyshev distance, and the Minkowski distance [31].

#### 4 Discussion and Experimental Results

The experiments were performed with several data sets using MATLAB. In the first stage of the proposed system, the iris ring is isolated from the input eye image. Segmentation is achieved here using the Integro-differential operator. Figure 5 shows a noisy iris detected by the proposed system. The figure shows circles overlaying the iris inner and outer borders.

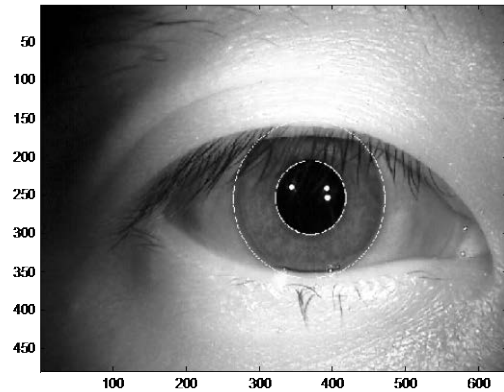


Figure 5: Segmentation of a noisy iris image

In the proposed system, after the iris is detected, it is normalized. Normalization is achieved here in two stages. In the first stage, the image representing the iris region is converted to a vector. For example, let the segmented iris region be defined by the matrix

$$s = \begin{bmatrix} a_{11} & a_{12} & a_{13} \\ a_{21} & a_{22} & a_{23} \end{bmatrix}$$

The corresponding iris vector  $n$  is then found by first converting the matrix  $s$  to a vector as follows

$$n = [a_{11} \ a_{12} \ a_{13} \ a_{21} \ a_{22} \ a_{23}]$$

Iris vectors have variable lengths depending on the input eye image. In the second stage of the normalization process, all iris vectors are forced to have the same length. This is achieved by truncating all iris vectors so that their lengths are equal to the length of the smallest iris vector belonging to the dataset under study. The truncation process ensures that the iris vectors can be suitably presented to an ANN after being transformed by the WPD, the next stage in the proposed system. All input vectors to an ANN must have the same dimension. Figure 6 depicts the lengths of the iris vectors in our dataset. It shows that the maximum and minimum lengths of the iris vectors are 34609 and 29510 (coefficients), respectively. Thus, to normalize the dataset, all iris vectors are truncated to have 29510 coefficients.

The normalized vectors are then transformed using a WPD that employs the dB1 wavelet. The transformation yields

approximation and detail vectors. In the proposed system, we retain the approximation coefficients and discard the detail coefficients since they carry a small portion of the signal energy. Figure 7 shows the average of the approximation vectors corresponding to iris vectors of four classes. Each class had 20 samples.

It can be seen from Figure 7 that approximation vectors of different classes have different peak values and different peak locations. We exploit this characteristic of the WPD transform to obtain distinctive features. Specifically, the proposed scanning technique is applied to the approximation coefficients to obtain the feature vectors. In the last stage of the proposed system,  $f$  is applied to an ANN for classification.

In the experiments, we test the performance of the proposed ANN system and the VQ system versus decomposition and threshold levels. Moreover, the proposed system is tested as a function of the number of neurons used. The VQ system used

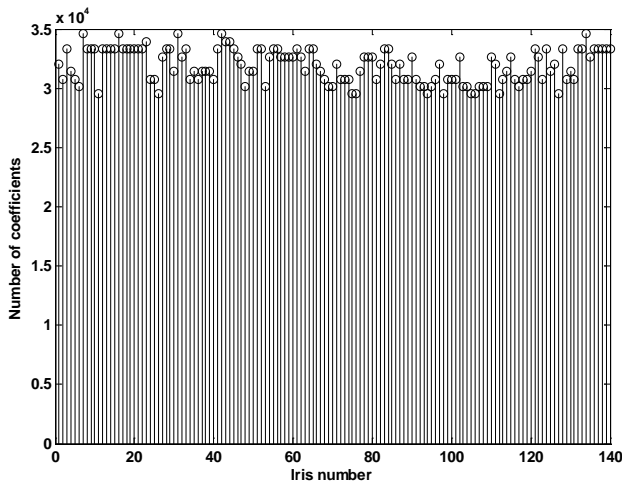


Figure 6: Lengths of the iris vectors for 7 classes with 20 irises per class

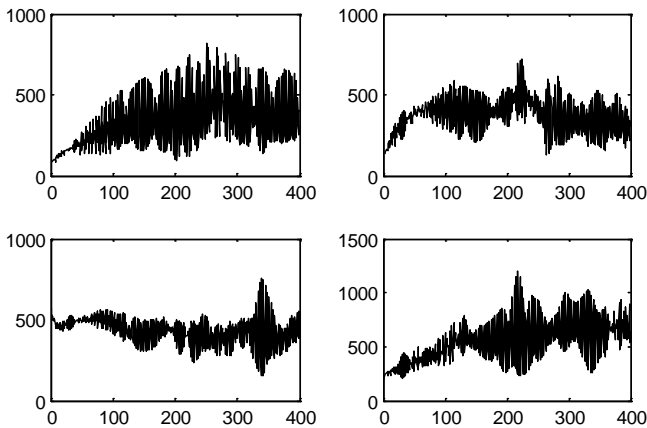


Figure 7: Average of approximation coefficients at level 6, for four iris classes (20 samples per class), using the dB1 wavelet

in the experiments employs the Euclidean distance.

In the first experiment (Figure 8), we test the error rate of the proposed ANN system versus wavelet decomposition level and number of neurons used in the first layer. The system employs the dB1 wavelet and the output (second) layer has 7 neurons corresponding to the number of classes. Figure 8 shows that the proposed system exhibits a minimum error rate of 5% when the decomposition level is 8 and the number of neurons is 11.

In the second experiment (Figure 9), we examine the error rates of the proposed ANN and VQ systems versus wavelet decomposition level, using the dB 1 wavelet. Here, the approximation vectors are presented to both systems without thresholding and the NN system used 10 neurons in the first layer. Figure 9 shows that the ANN system outperforms the VQ system and produces a low error rate of 5% (when the decomposition level is 8) while the lowest error rate for the VQ system is 43.57% (obtained when the decomposition level is 10). The highest error rate for both systems occurs when the decomposition level is at its maximum value of 14.

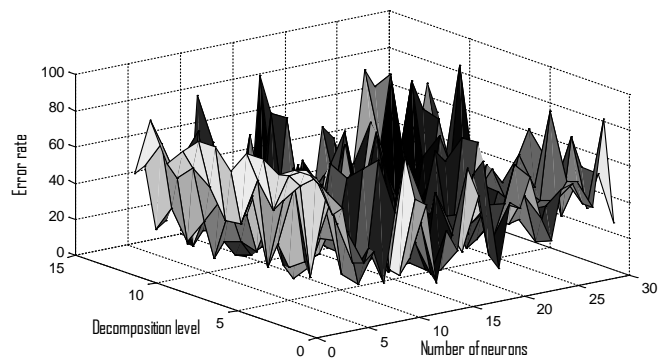


Figure 8: Error rate of the ANN system vs. decomposition level and number of neuron

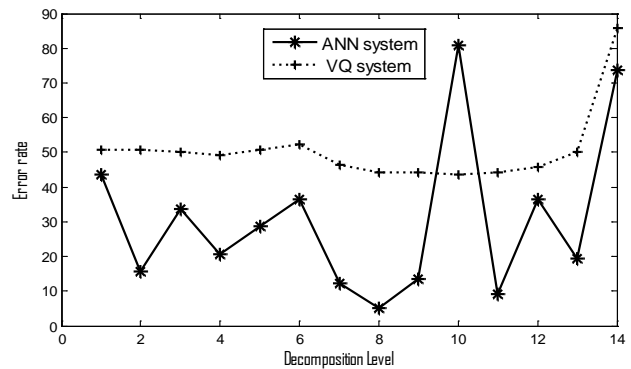


Figure 9: Error rate for the ANN and VQ systems versus decomposition level

In the last experiment (Figure 10), we test the performance of the VQ system as a function of both threshold level and decomposition level. Figure 10 shows that that the VQ system

has a minimum error rate of 32.14% when the wavelet decomposition level is three and the threshold level is 78.

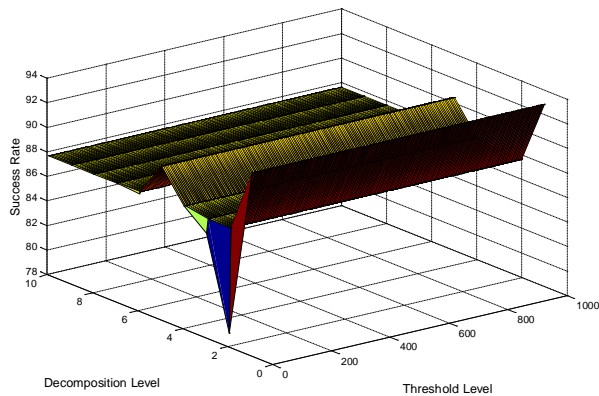


Figure 10 Error rate of the VQ system versus decomposition level and threshold level

### 5 Implementation of the Proposed Method

The iris recognition scheme proposed here (Figure 2) requires as input an iris image. The image can come from a database for off-line processing. For online or real-time processing, a scanner, such as the one shown in Figure 11, must be used to obtain the iris image from the target object (person).

The remaining key steps used in the proposed system in order to go from an image of a person's eye to positively identifying that person are: segmentation, template generation and template matching.

The segmentation, Wavelet transformation and classification algorithms use digital signal and image processors such as the one shown in Figure 12.



Figure 11: Iris recognition camera [9]



Figure 12: DSP processor [10]

A DSP processor is a specialized microprocessor (or a SIP block), with its architecture optimized for the operational needs of digital signal processing. The goal of DSPs is usually to measure, filter, and/or compress continuous real-world analog signals.

Here, the computation speed of the system is clearly dependent on the speed of the scanner and DSP processor and the accompanying hardware.

The proposed algorithm can take substantial processing time in software on the order of a few hundred million operations.

### 6 Conclusion

Presented in this paper is a new approach to iris classification. In the proposed system, the iris is first extracted from the input eye image using the integro-differential operator. The isolated iris disc is converted to a 1-D vector and then normalized so that all the irises in the dataset have the same length. The 1-D WPD is used to transform the normalized iris vector in order to reduce its dimension and simplify the subsequent feature extraction stage. Relying on the fact that the low-frequency components of a signal carry most of the information about the signal, certain approximation coefficients are scanned as features using a novel thresholding technique that keeps the values and locations of the high-magnitude approximation coefficients. The selected features are then applied to an ANN for classification.

The proposed system has various configurations and parameters. In this study, we investigated the optimum ANN structure, the optimum WPD parameters, and the optimum threshold level for iris recognition. To show the robustness and the validity of the proposed system, its performance is compared to that of VQ, a minimum-distance classifier that employs the Euclidean distance. Both the proposed system and the VQ system receive the same feature vectors as input. Simulation results prove that the proposed ANN system produces a low error rate of 5% and always outperforms VQ system.

## References

- [1] Cairo Amman bank, <http://www.cab.jo>, 2008.
- [2] CBSR, Center for Biometrics and Security Research, <<http://www.cbsr.ia.ac.cn/english/Databases.asp>>, 2005.
- [3] R. Clarke, "Human Identification in Information Systems: Management, Challenges, and Public Policy Issues," *Information Technology & People*, 7(4):6-37, 1994.
- [4] J. Daugman, "High Confidence Visual Recognition of Persons by a Test of Statistical Independence," *IEEE Transactions on Pattern Analysis and Machine Intelligence*, 15(11):1148-1161, 1993.
- [5] J. Daugman, "Statistical Richness of Visual Phase Information: Update on Recognizing Persons by Iris Patterns," *International Journal on Computer Vision*, 45(1):25-38, 2001.
- [6] J. Daugman, "Probing the Uniqueness and Randomness of Iris Codes: Results from 200 Billion Iris Pair Comparisons," *Proc. IEEE*, 94(11):1927-1935, 2006.
- [7] R. O.Duda and P. E. Hart, "Use of the Hough Transformation to Detect Lines and Curves in Pictures," *Communications of the ACM*, 15:11-15, 1972.
- [8] P. V .C. Hough, "Machine Analysis of Bubble Chamber Pictures," *Proc. Int. Conf. High Energy Accelerators and Instrumentation*, 1959.
- [9] <http://www.m2sys.com/wp-content/uploads/2014/04/M2-AutoTilt-Iris-Camera-icon.png>, 2004.
- [10] [http://www.differencebetween.info/sites/default/files/images/2/dsp-processor\(1\).jpg](http://www.differencebetween.info/sites/default/files/images/2/dsp-processor(1).jpg), 2015.
- [11] IITDirisdatabase, <<http://web.iitd.ac.in/biometrics/Data-baseIris.htm>>, 2008.
- [12] R. W. Ives, D. A. Bishop, Y. Du, and C. Belcher, "Iris Recognition: The Consequences of Image Compression," *EURASIP Journal on Advances in Signal Processing*, 2004(1):304-316, 2010.
- [13] H. B. Kekre, S. D. Thepade, J. Jain, and N.Agrawal, "IRIS Recognition using Texture Features Extracted from Haarlet Pyramid," *International Journal of Computer Applications*, 11(12):1-5, 2010.
- [14] National Institute of Standards and Technology, Iris Challenge Evaluation, Available from: <http://iris.nist.gov/ICE>, 2006.
- [15] E. Newham, "The Biometric Report," <<http://www.sjb.com/>: SJB Services>, New York, 1995.
- [16] Palacky University Iris Database, Available from <http://www.advancedsourcecode.com/irisdatabase.asp>, 2010.
- [17] P. J. Phillips, W.T. Scruggs, A.J. O'Toole, P.J. Flynn, K.W. Bowyer, C.L. Schott, and M. Sharpe, "FRVT 2006 and ICE 2006 Large-Scale Results," Technical Report, National Institute of Standards and Technology, NISTIR 7408, Available from: <<http://iris.nist.gov/ice>>, March 2007.
- [18] H. Proença, "An Iris Recognition Approach Through Structural Pattern Analysis Methods," *Expert Systems*, 27(3):146-155, 2010.
- [19] H. Proenca and L. A. Alexandre, "UBIRIS: A Noisy Iris Image Database," 13<sup>th</sup> International Conference on Image Analysis and Processing (ICIAP2005), pp. 970-977. Available from: <<http://iris.di.ubi.pt>>, September 2005.
- [20] H. Proenca and L. A. Alexandre, "Iris Segmentation Methodology for Non-Cooperative Recognition," *IEE Proceedings on Vision, Image and Signal Processing*, 153: 199-205, April 2006.
- [21] A. M. Sarhan, "Optimal Statistical Artificial Neural Networks for Arabic Character Recognition," *Proceedings of 16th Int'l Conference on Computers and Their Applications*, Cancun, Mexico, pp. 53-58, April, 2008.
- [22] A. M. Sarhan, "Iris Recognition using the Discrete Cosine Transform and Artificial Neural Networks," *Journal of Computer Science*, 5(5):369-373, 2009.
- [23] A. M. Sarhan, "Cancer Classification Based on Microarray Gene Expression Data using DCT and ANN," *Journal of Theoretical and Applied Information Technology (JATIT)*, 6(2):208-216, 2009.
- [24] A. M. Sarhan, "A Comparison of Vector Quantization and Artificial Neural Network Techniques in Typed Arabic Character Recognition," *International Journal of Applied Engineering Research*, 4(5):805-817, 2009.
- [25] A. M. Sarhan, "A Novel Gene-Based Cancer Diagnosis with Wavelets and Support Vector Machines," *European Journal of Scientific Research*, 46(4):488-502, 2010.
- [26] A. M. Sarhan, "Cancer Classification Based on DNA Microarray Data using Cosine Transform and Vector Quantization," *International Journal of Computers and Their Applications*, 17(4):212-223, 2010.
- [27] A. M. Sarhan, "Wavelet-Based Feature Extraction for DNA Microarray Classification," *Artificial Intelligence Review (AIR)*, 39(3):237-249, 2013.
- [28] A. M. Sarhan, "A WPD Scanning Technique for Iris Recognition," *International Journal of Computer Applications*, 85(14):6-12, January 2014.
- [29] A. M. Sarhan and O. I. Al-Helalat, "Probabilistic Artificial Neural Networks for Arabic Character Recognition," *Proceedings of 16th Int'l Conference on Software Engineering and Data Engineering*, Las Vegas, pp. 131-136, July 2007.
- [30] A. M. Sarhan and O. I. Al-Helalat, "Arabic Character Recognition using Artificial Neural Networks and Statistical Analysis," *Proceedings of the ICCESSE Conference*, pp. 32-36, May 2007.
- [31] A. M. Sarhan and O. I. Al-Helalat, "A novel approach to Arabic characters recognition using a minimum distance classifier," In *Proceedings of the World Congress on Engineering*, London, U.K, pp. 679-684, July 2007.
- [32] M. Vatsa, R. Singh, and P. Gupta, "Comparison of Iris Recognition Algorithms," *International Conference on Intelligent Sensing and Information Processing*, pp. 354-358, 2004.
- [33] Z. Wei, T. Tan, and Z. Sun, "Synthesis of Large Realistic Iris Databases using Patch-Based Sampling," *Proc. Int. Conf. Pattern Recognition*, pp.1-4, 2008.



**Khalid A. Buragga** is an Associate Professor in the faculty of Computing and Information Technology at Northern Border University in Saudi Arabia, where he also holds the position of Vice President for Academic Affairs. Dr. Buragga received his B.Sc. in Computer Information Systems from King Faisal University and received his M.Sc. in

Computer Information Systems from University of Miami, USA. Dr. Buragga obtained his Ph.D. in Information Technology from George Mason University, USA. His research interests include software design, software development, software quality, software reliability, E-Commerce and web development, Business Process Re-engineering, communications, networking and signal processing.



**Sultan Aljahdali**, Ph.D. is a Professor of Computer Science in the College of Computers and Information Technology at Taif University, Taif, Saudi Arabia. Prof. Aljahdali obtained a Ph.D. in Information Technology from George Mason University, USA in 2003, and completed a Leadership

Program at Harvard Business School, Harvard University, Boston, USA in 2013. He received his B.S from Winona State University and M.S. with honor from Minnesota State University in Mankato. Prof. Aljahdali has made research contributions on software testing, developing Software Reliability Models, Soft Computing for Software Engineering, Computer Security, Reverse Engineering and Medical Imaging. He is an author or co-author of more than 100 peer reviewed academic publications. Prof. Aljahdali is a member of several professional societies including ACM, IEEE, ACS and ISCA.



**Ahmad M. Sarhan** was born in Jordan in 1970. He received a B.S. in Biomedical Engineering from Syracuse University, NY, USA in 1991, M.S. in Electrical Engineering from Syracuse University in 1992, and a Ph.D. in Electrical Engineering from the University of Dayton, Ohio, USA in 1996. He is currently a Full Professor of Computer Engineering

at Taif University in Saudi Arabia. Before joining Taif University, Prof. Sarhan had worked at several universities including New York Institute of Technology, the University of Dayton, King Faisal University, Yarmouk University, the University of Jordan, and Amman University. Prof. Sarhan has also worked at several universities in the United Arab Emirates, including Ajman University, the Higher Colleges of Technology, the Naval College, and Ajman University. Prof. Sarhan also worked in the industry as an executive manager of a medical company in Dubai, UAE. Prof. Sarhan received several awards including, The Best Student Paper Award for the paper "Partition-Based Filters," the Most Outstanding Paper published in the NAECON Conference, Dayton, Ohio, May 1995 and the award by the United Nations Development Fund for Women (UNIFEM) for supervising The Best Female Student Project, Jordan, 2009. Dr. Sarhan received a tuition scholarship from Syracuse University, USA and a teaching and research assistantship from the University of Dayton, USA. Prof. Sarhan's main research interests include adaptive signal processing, pattern recognition, and biomedical signal processing.



**Marcel Karam** received his Ph.D. in Computer Science from Dalhousie University in 2002. He is currently an Associate Professor in the Department of Computer Science at the American University of Beirut. Dr. Karam's primary research track aims at providing end-users with techniques and tools to improve the quality and efficiency of the

many facets that comprise the software engineering.

# Using Genetic Algorithm & Neural Network for Modeling Learning Behavior in a Multi-Agent System during Emergency Evacuation\*

Sharad Sharma<sup>†</sup> and Kolawole Ogunlana<sup>†</sup>  
Bowie State University, Bowie, Maryland, 20715, USA

## Abstract

It is expensive and time consuming for emergency personnel to perform multiple evacuation drills in real time for a building. One cannot gain knowledge to improve the design and layout of future buildings without running multiple drills. We have implemented a goal finding evacuation simulation application to help run multiple evacuation drills and hypothetical scenarios. This paper investigates agents' behavior during emergency evacuation scenarios in a goal finding application. We have modeled learning and adaptive behavior which includes individual and collective behaviors. The adaptive behavior focuses on the individual agents changing their behavior in the environment. The collective behavior of the agent focuses on the crowd-modeling and emergency behavior in the goal-finding application. We have developed new intelligent agent based characteristics such as autonomy, social ability, cooperativeness, and learning ability which define their final behavior when trying to reach a goal. The contributions of this paper lie in our approach of combining Genetic Algorithm (GA) and Neural Network (NN) to show learning and adaptive behavior of agents in a goal finding application. The proposed application will aid in running multiple evacuation drills for what-if scenarios by incorporating agent characteristics. We can say with standard error of fixed value 0.1, 95% confidence level and standard deviation 1.0 that the average time for occupants to evacuate performed slightly better at the lower range of number of occupants (10 – 50) compared to the other pathfinder simulator.

**Key Words:** Genetic algorithm, emergency evacuation, neural network, agent-based evacuation, models, multi-perception.

## 1 INTRODUCTION

A model or simulation provides us the ability to perform various tasks seen in the real world. For example, without

models, it is very expensive and time consuming to simulate an emergency evacuation in an airplane or a building. The objective of this paper is to propose a model for simulating agent behavior in a goal-finding application using an algorithm based on genetic and neural networks that includes agent behavior characteristics. In order to simulate airplane evacuation, there is a need for access to a real size plane, recruiting sample passengers, pilots, flight attendants, and crew members. Sharma [13-14, 18-20] explained the renewed use of Agent-Based Modeling and Simulation (ABMS). Intelligent agents can be used by students interested in other applications like teaching kids how to safely cross busy intersections, providing online instructions in a university and giving military and medical personnel valuable experience they may face in performing their professions. Sharma further explained that using an accurate simulation model is very important, especially in emergency evacuation scenarios [18]. The accuracy is even more important in a simulation where results can change as various parameters are changed. For example, psychological parameters of anger, stress, and panic would have to be accurately observed in an emergency evacuation in the real world. Favorite goals and sub-goals [15] have been used by Sharma for simulating agent behavior in a disaster evacuation multi-agent system.

This paper examines how to simulate evacuation of a building structure while observing the perception and cognition of the intelligent agents in a goal-finding application. In the beginning of an architectural project, for example, the designer of a building usually has to plan and strategize how to make the space usable and efficient for the people using the facility. The decisions made by the designer will affect the future behavior of the people that will move through the building or airplane structure to be constructed. The designer would benefit from having an application that would help to connect the way people behave and the factors considered in construction of a building structure. How do we test whether this application precisely simulates the navigation of people when developing a structure? Consequently, an investigational device that can be used to model people's progress through a path and the way they behave in various scenarios they face, is projected and to be developed. This device will provide wise methods for re-tooling the pattern and the layout of building meeting places and will direct designers on achieving a higher probability of

\* Extended paper from Proceedings at the ISCA 30th International Conference on Computers and their Applications (CATA 2015), Honolulu, Hawaii, USA, March 9-11, 2015

<sup>†</sup> Department of Computer Science. Email: {ssharma, ogunlanak0415}@bowiestate.edu.

efficient and maximized use of these structures. A prototype application was developed (refer to Figure 1) that uses an existing building layout to demonstrate the multilayer perceptron simulation. In addition, more prototype applications showing the simulation functionalities of the planned evacuation representation to display the way people behave and their thought process for a building evacuation is also shown.

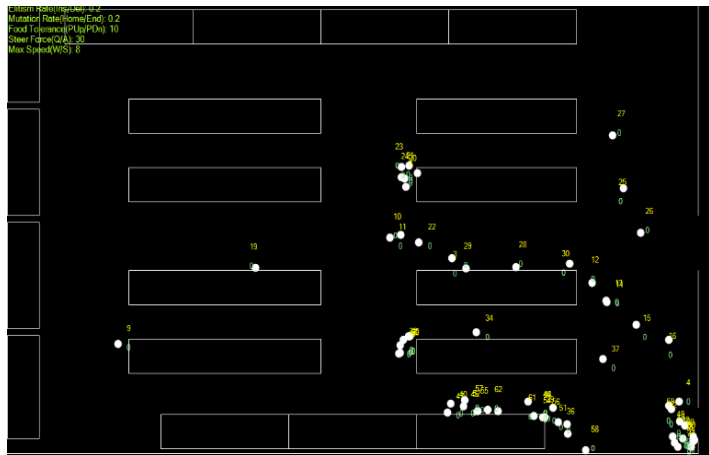


Figure 1: Agents evacuating in a multi-agent system

The focus of this paper is to study human behavior and human reactions in an emergency situation like evacuation. We have shown learning behavior and adaptive behavior using a genetic algorithm and neural network in a multi-agent system. The rest of the paper is structured as follows: Section 2 briefly describes the work done previously. Section 3 describes the multi-agent system. Section 4 illustrates the proposed navigational algorithm and describes the navigation and simulation results. Section 5 lists conclusion and future work.

## 2 Related Work

The ability to model agent behavior in the decision making ability of agents when they are evacuating is very important, especially when creating an environment that represents the real world. Three ways that were used to represent the real world by other researchers like Chooramun include coarse networks (Pedroute), fine network (buildingExodus), and continuous (Simulex) [16]. Each of these methods of representing the real world proposed by Chooramun has their advantages and disadvantages that led to their combination in the hybrid spatial discretisation (HSD) method [16]. The coarse networks increase the pace of the agents in the vague or less detailed areas that are needed in the modelled environment. Fine networks pickups up the load for rendering areas in the environment where there are a lot of interactions between agents. Lastly, the continuous is used where more detail is needed to be captured in the agent to agent interactions in the environment. Once a method such as HSD has been selected for modelling the physical environment, the next step

would be to select the way the results of the evacuation would be analyzed by the researcher. The three ways of analysing evacuation put forth by Gwynne are through simulations, optimization and risk assessment [4]. Simulations, on one hand, focus on modelling the point to point movements of the agents and their behaviors as they search for exits in the evacuation. Unlike simulations, Gwynne explained that optimization is built on the premise that agents would move as a group to evacuate together in one direction without attempting to notice other obstacles and parts of the environment [4]. Risk assessments take a different approach with agents affected by environmental factors like fires, smoke and reduced visibility, resulting in the risk of not finding the exit. The behavior of the agents in each of the analyses proposed by Gwynne may be affected by artificial intelligence, rules, implicit matches, and functionality [4].

Artificial intelligence tries to replicate human intelligence in the evacuation [7]. Rules use “if-then” conditions of the environment faced by the agent to control their reactions. Implicit matches’ identifiers are assigned to agents to control how fast or slow their movement is while evacuating [7]. Lastly, functional uses physics equations, for example, to control the movement of the agents. The movement of agents can be taken into account when designing buildings. The safety of a building design can be measured against the number of fires in similar designs against the number of people that were hurt in such an incident [7]. The data when plotted on a graph is referred to as the F-N plot. The F-N plot usually captures the three kinds of evacuation crowd behaviors, which are individual, individual to individual and groups [7]. Individual behavior is based on following past knowledge of where exits are located when evacuating. It also involves other individuals following the instructions of a leader who they perceive has knowledge of exits during evacuation [7]. The probability of individual to individual interaction through pushing or a stampede increases with panic. The negative effect of panic also increases as the size of the group that is trying to evacuate grows in a building [7]. The perception of panic starts the behavior process of individuals when deciding what situations should cause them to evacuate and what steps to take to evacuate and then to actually evacuate [7]. The time it takes to begin the evacuation is important to track and involves predetermined movement time, taking a walk calculating speed, passenger attributes, taking steps and choosing the exit [24]. Exit choice decisions are usually based on the particular locations that individuals have knowledge of before the emergency [22]. Sometimes the exit chosen by the individual trying to evacuate may not be the closest but another better one may be picked if the individual can see beyond the exit [22]. Also, verbal evacuation directions are better than alarm rings when trying to get people to start moving towards an exit. Other psychological factors that affect an individual’s ability to find an exit after receiving verbal warning are worrying, overburdened with too much task, task difficulty, significant task, tiredness and worldly factors [1]. These factors that affect the speed of individuals as they move from

one area to another towards an exit can be combined into a space compressed object (SCO) [8]. The SCO would involve utilizing powerful computers to track the various factors in the simulation [21].

Multi-Layer Perceptrons (MLP) contain hidden layers that increase the area of theories that the network can symbolize, which means the number of problems it can solve is very large [17]. MLPs use genetic algorithms to generate the weights for the input which are fed into the neural network to generate the output. This allows it to continually adjust the MLP to reduce the error as it searches for the solution to the problem it is trying to solve. Individual hidden neurons signify a perceptron that points to a lenient threshold function within the input space. The output neuron derives its value from leniently adding together the various threshold functions from the input space. When we adjust the weights in MLPs, we change the function in the network and learning, such as classification or regression, is achieved. Its structure and training is well developed and has a good generalization capability.

### 2.1 MLP

The advantages of MLP are that it is a fast and accurate model of an original problem (continuous and integrable functions) it learned after training [11]. It also distributes the work of learning with the combination of many neurons responding to many external inputs which either turns it off, on, or in transition state. The disadvantages of MLP are that sufficient training data is required, which could be large for high dimensional problems, and that it also has too many or too little hidden neurons, which may lead to overlearning or under learning, respectively.

### 2.2 Radial Basis Function (RBF)

The advantages of RBF are that RBF provides better initial values for hidden neuron centers using unsupervised training sample distribution compared to random weight [11], and it also learns at faster rates and shows reduced sensitivity to the order of presentation of data. It makes them good for problems with a small number of inputs. It works better when training data is large and sufficient. The disadvantages of RBF are that when the amount of training data becomes minimized, it degrades faster compared to MLP and it also does not have a better generalization capability compared to MLP.

### 2.3 Wavelet

The advantages of wavelet are that the wavelet reduction algorithm can selectively choose wavelets that best fit the training data [11] and it also has a network of weight parameters that can be refined using supervised training combined with wavelets functions that match data output. The disadvantages of wavelet are that the unnecessary large number of initial wavelets can be created in a lattice approach, which leads to redundancy. Also, performance degradation may occur

because of large numbers of hidden neurons affecting training.

### 2.4 Arbitrary Structures

The advantages of arbitrary structures are that they have a flexible structure not layered, so all neurons can be connected to all other neurons [11] and it also has external output and input that can be applied to and from any predefined set of neurons. The disadvantages are that the complexity increases between the links among the various neurons and they have to manage optimization of added/deleted neurons and connections between training.

### 2.5 Self-Organizing Maps (SOM)

The advantages of SOM are that they facilitate automatic decomposition through processing and learning of training data [25] and it is also useful in the case where the problem is complicated and the precise shape of subspace boundaries are not easy to determine. The disadvantages of SOM are that sufficient training data is required similar to a clustering algorithm and it can also be dependent on MLP to provide input.

### 2.6 Recurrent

The advantage of recurrent is that it allows time-domain behaviors of a dynamic system to be modeled [25]. The disadvantage of recurrent is that it depends on the history of system states and inputs, and thereby a mechanism must be available to capture and save the history.

Multiple games have utilized the neural approach [5] for learning behavior in agents. Sharma et al. [6, 16] compared their tool with an existing commercial evacuation tool for accuracy, building traffic characteristics, and cumulative number of people exiting during evacuation. There are a number of evacuation softwares that have been constructed such as buildingEXODUS [3], simulex [23], AvatarSim [13], and EvacSim [9]. Our proposed application is similar to them and is capable of simulating people looking for exits. The buildingEXODUS software focuses on the interfacing of people, how people are organized, and the way people are located in their world.

## 3 Characteristic of Multi-Agent System

In a multi-agent system, the agents follow the common definition of agents, such as:

- Ability to communicate with other agents,
- hold its own resources: state and behavior,
- hold representation of the environment,
- act on the environment,
- can reproduce itself and
- local representation of the environment.

Our proposed multi agent system models human behavior. The agent characteristics include attributes, emotions, memory, rules of behavior and learning, and decision making capabilities. Our proposed multi agent system also uses MLP (refer Figure 2) and consists of variables which provide a way to keep existing the state as it moves, thereby relying on the stimulus it receives from the world. The data of the agent is saved as shown below:

- A. Location of agent (x and y coordinates),
- B. Direction of agent,
- C. Distance of agent (from current location to closest exit),
- D. Speed of agent,
- E. Mass of agent,
- F. Force exerted by agent,
- G. Max Force agent can attain,
- H. Agent Number unique identifier of agent,
- I. Net is private neural network of agent,

- J. MyWorld is the private copy of the static environment in which the simulation is done,
- K. Exit reached array,
- L. Invisible flag used to display agent in environment, and
- M. Agent Type is hostile or non-hostile.

### 3.1. Simulation

The simulation follows a certain sequence which is outlined in the steps below:

- i. Simulation is timed and tracked to see which people are closest to the exit using the brain (the NN) in an iteration which takes 10-12 seconds. People closest to the exit have the highest fitness value, while people furthest away from the exit have the lowest fitness value.
- ii. The GA's roulette wheel selection is used to select the best people (highest fitness) to be parent to children

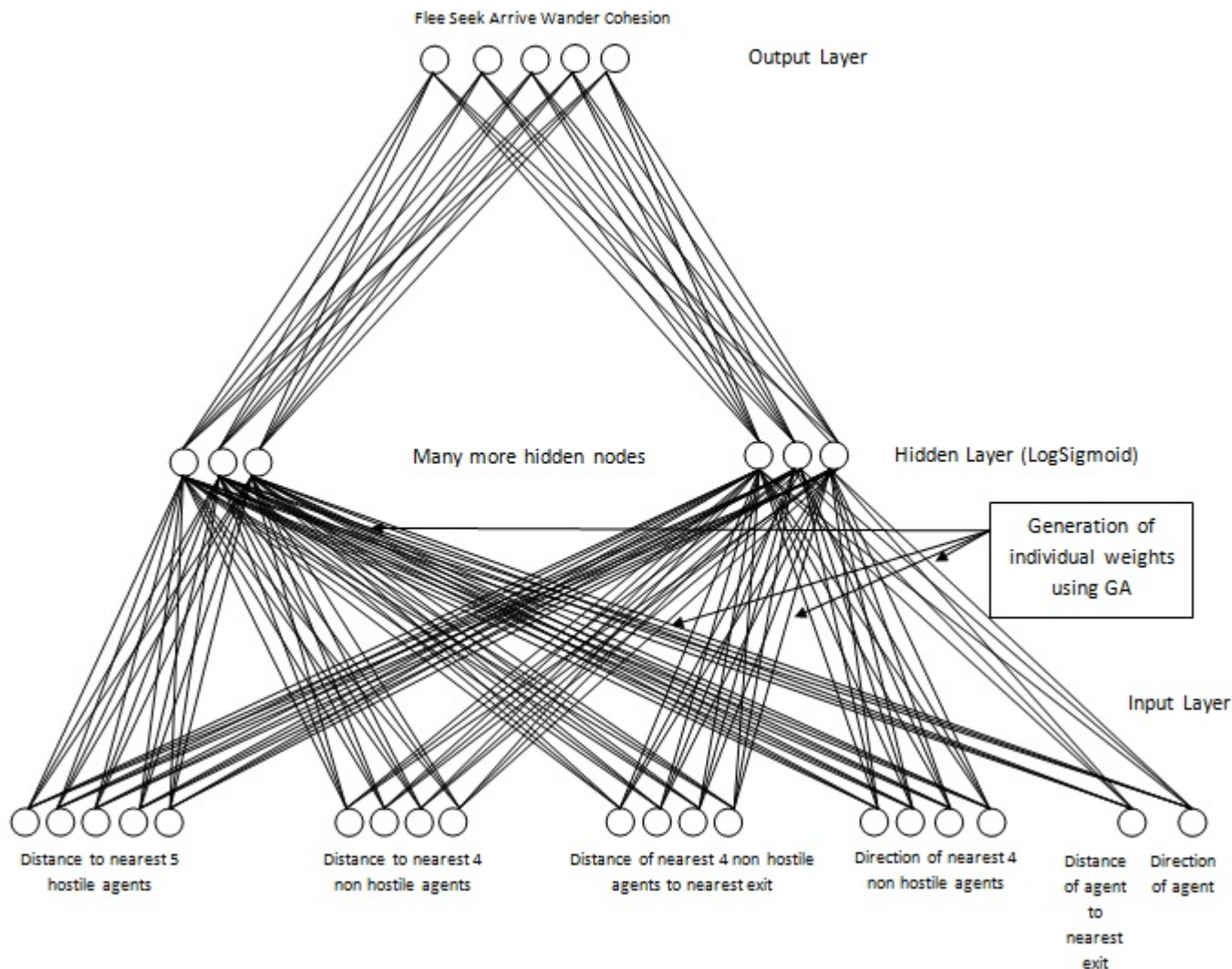


Figure 2: Multi perceptron network

(lower fitness) to help them to get closer to the exit. This is done by summing all the fitness values ( $S$ ) of all people and using a random value ( $r$ ) between 0 and  $S$  to select the first parent fitness value whose sum “ $s$ ” is greater than “ $r$ ”. This is done twice to select two parents. Other researchers have used Rank, Steady State and Elitism to speed up or increase performance of roulette wheel selection.

- iii. Parents’ weights are then mutated by making random changes to random weight locations.
- iv. Children are then initialized with the weights of the parents.
- v. Once all people have exited the building, the simulation ends. The simulation contains static obstacles (tables in computer lab) and dynamic obstacles (other people).

### 3.2 Agent Visualization

A black box in the environment represents the exit with the time tracking of how long it takes in the simulation to reach the exit. Each agent has different colors based on the level of panic.

The color of the agent is red which means extreme panic behavior and reduces the speed of the agent getting to the exit. White means low level of panic. The training data is generated using an initial set of 20 to 100 scenarios read from an input file; each one is a set of inputs with the output we would like to see. We split the scenarios into two groups: a training set (used to do the learning) and a testing set (used to check on how learning is going). Ten training and ten testing examples would be an absolute minimum for this problem. Usually, while you disperse a data set into a training set and testing set, the majority of the data is utilized for training, and a minority

percentage of the data is used for testing. An analysis must be done in random to make sure the testing and training sets are alike. By using comparable data for training and testing, you can reduce the chance of data inconsistencies and better comprehend the features of the model. If the network continually gets the test set wrong after training, it may mean that we need to add more training data.

### 3.3. Navigation

The navigation shown in Figure 3 starts with the agent finding the closest exit to their current location. This involves calculating the minimum distance to that exit. The next step is to set the MLP input of distance and direction of the agent which is then fed into the NN which outputs the direction and speed. The agent is then updated to the new direction, behavior and speed while also performing both static and dynamic obstacle avoidances. The agent then moves to the next position which involves updating its location. The simulation then checks if exit is reached; if yes, remove the agent from the environment and check if the agent is the last to exit the environment. If no, start again from the beginning of the navigation for other agents still in the world, else end the simulation.

## 4 Simulation and Results

For preliminary validation of our system, we did a set of small, proof-of-concept style experiments modeling an actual room used as a computer lab in our department building. This proof-of concept would allow us to study the complex interaction of agents in great detail in a single room and would be extended in the future to multiple room/building models.

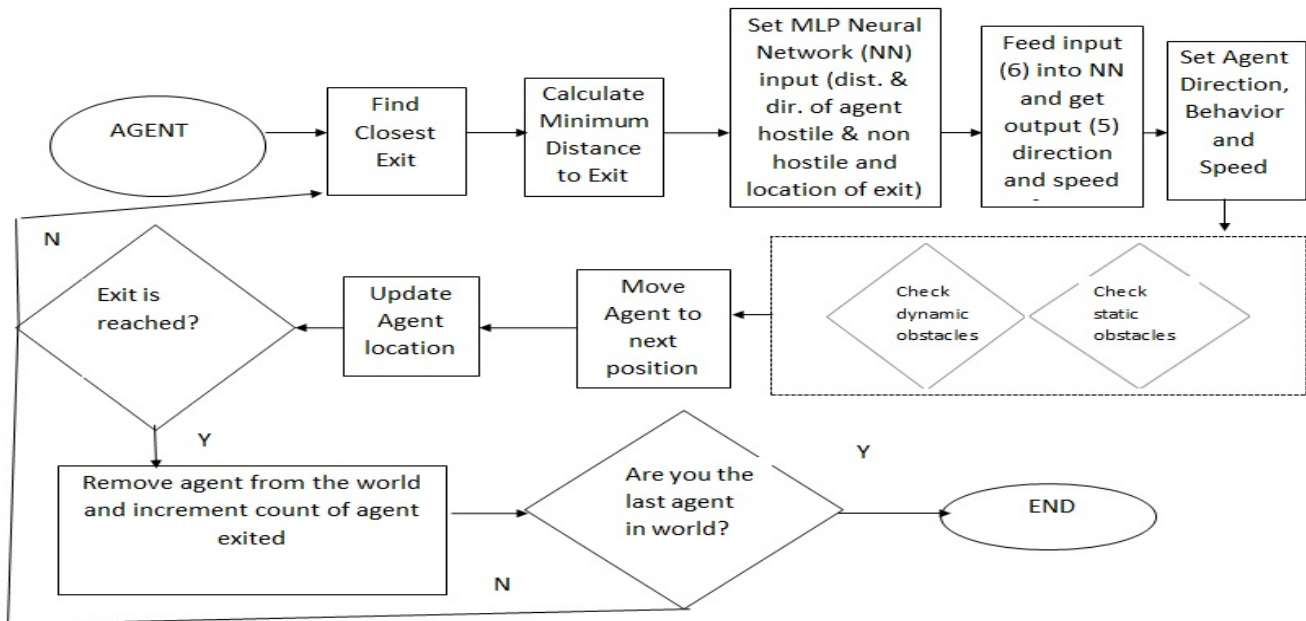


Figure 3: Agent navigation to exit

Our proposed application for emergency evacuation is written in Microsoft c-sharp (C#). Learning and adaptive behavior of agents is achieved by using GA & NN to perform automated testing in evacuation simulation.

The functionality would consist in the user designing a room, and then having the program run automatically a set of tests, varying the placement and number of agents, obstacles and exits. After a defined set of tests have taken place, the program would use the collected statistics to automatically determine optimal placement for fire exits, doors, etc. Our proposed C# application is shown in Figure 4 as generation and current best. The length of a generation is the time limit of 90 seconds after which the count of agents that have successfully evacuated are recorded in the current best. Walls and other obstacles in the application are shown as rectangles. Doors are represented as gaps in the wall. The parameters for drawing the walls are passed to the simulation through an input text file specified by the user of the application.

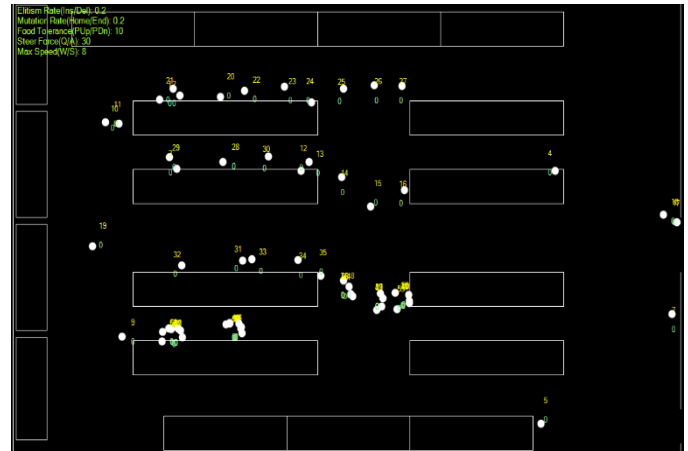


Figure 5: Initial Start of Simulation Screen

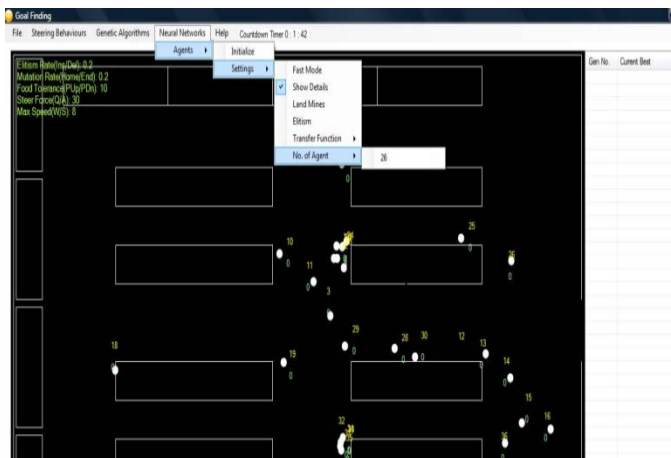


Figure 4: Intelligent agent graphical user Interface

### 4.1 MLP Algorithm GA & NN

An AI-controlled character makes use of 19 input values: the distance to the nearest 5 hostile agents, distance to the nearest 4 non hostile agents with their distance to nearest exit and direction values, and the distance to nearest exit and direction of the agent [5]. We assume five different output behaviors agents can exhibit on their way to an exit: flee, seek, arrive, and wander and cohesion, as shown in Figure 2.

We have used a network with three layers: input layer and output layer, plus an intermediate (hidden) layer. The input layer has the same number of nodes: 19. The output layer has the same number of nodes as there are possible outputs: 5. Hidden layers will have at least as many nodes as the input layer: 24. Figures 5 and 6 show the simulation screens during agent evacuation.

Steps: to begin, all the weights in the network (refer Figure 2) are set to small random values and a set of iterations of the learning algorithm is done involving selecting an example

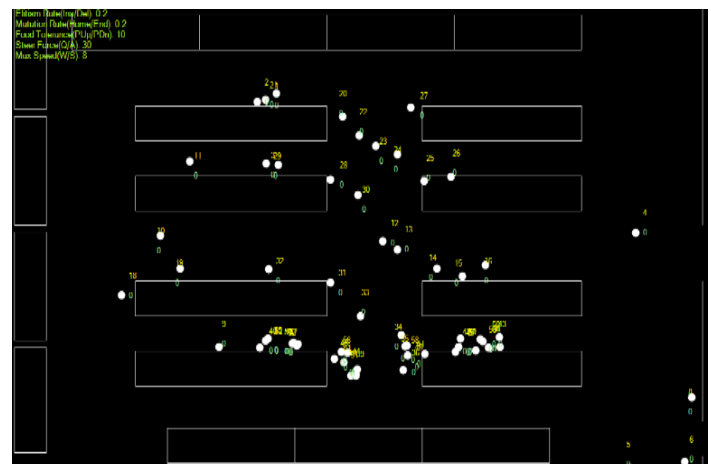


Figure 6: Second iteration of simulation screen

scenario from the training set. We then take the inputs fed forward to guess the output and change the network (back propagation) by comparing the expected output and the guess. Every 10 – 15 seconds the GA roulette wheel selection process is used to select the two parents that will be used to change the weight of the children. After iterations are done, we can check to see if learning is done by running on the test group of examples. If the guess output aligns with our expectations, NN has learned properly, else we can run more training on the network.

Figures 5 and 6 depict a lecture hall where there are 50 agents. Each agent’s behavioral characteristics as well as group characteristics are defined through the input file. Agents in the C# application are drawn as circles in the simulation. The application has one simulation mode where agents steer themselves, so they do not pass through other agents.

### 4.2 Evaluation

The smart agent simulator for disaster evacuation is written in Microsoft c-sharp. It functions comparable to Pathfinder

2014 established by Thunderhead Engineering for agent centered egress modeling. The smart and Pathfinder simulators both have a graphical user interface for modelling and planning. Smart simulator is capable of 2D conception for outcome exploration while Pathfinder has 2D and 3D (Figures 6 and 7). Pathfinder was chosen as the application for comparison with the smart agent simulator because of the ease of use in creating a simulation environment and ability to assess evacuation mockups more rapidly and yield more accurate illustrations. Output of the intelligent application is shown to the right in Figure 4 above as cohort and current best. The measurement of a cohort is 90 seconds, after which the agents are calculated that have effectively evacuated and are documented in the existing best. The environment that the agent will transverse in the smart simulator is a 2D rectangle (Figure 6) demonstrating the proportions of the room. Measurements of the room are denoted on the monitor with a rectangle width 1015 and height 695 pixels. The aggregate quantity of people modeled in the test simulation is about 45.

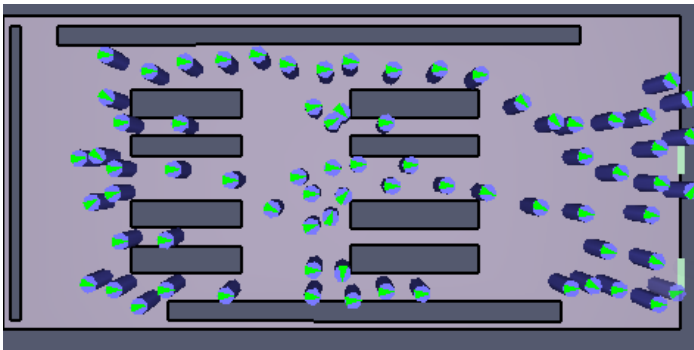


Figure 7: Pathfinder graphical user interface

Walls and other obstacles in the smart simulator are shown as rectangles that cannot be walked through by the agents. Doors are characterized as openings in the fence. The considerations for representation of the walls are passed to the smart simulation through an input text file indicated by the manipulator of the simulator. Pathfinder characterizes the movement environment with a neighboring lattice resembling the building. Openings in the surrounding mesh show the demonstrations on the walls and areas that cannot be passed by the occupants. Doors are characterized by unique boundaries in the direction-finding mesh. Stairways and elevators can also be represented in the pathfinder simulator. The flexibility in the movement simulation is combined to provide a dominant simulation device with malleable switch over inhabitants and performance to bring improved consequences. Pathfinder can import AutoCAD format DXF and DWG files to swiftly use the introduced geometry to describe the inhabitant walking cosmos for the evacuation model. PyroSim or Fire Dynamics Simulator (FDS) models can also be used to abstract the walking universe. If you have a blueprint, it can be introduced in GIF, JPG, or PNG format and then used as a contextual to help you speedily draw your model directly over the image.

Triangulation also assists constant drive of folks throughout the typical environment, likened to other simulators that split the cosmos into cells that can exaggeratedly constrain the movement of occupants. Pathfinder cares for two replication approaches. In Piloting mode, agents proceed independently to their objective, while dodging other tenants and difficulties. Door flow rates are not specified but result from the interaction of occupants with each other and with boundaries. In Society of Fire Protection Engineers (SFPE) mode, agents use behaviors that follow SFPE guidelines, with density-dependent walking speeds and flow limits to doors. SFPE results provide a useful standard for evaluation with other outcomes, but SFPE calculations do not prevent many individuals subjugating the similar space. Optionally, Pathfinder approves to decide door drive amounts in steering method to gain greater conception in a controlled ideal. You can effortlessly control among methods in the Pathfinder user interface. By default, each inhabitant (agent) produces a mixture of constraints to hand-pick their present pathway to an exit. The constraints include: file intervals for each entry of the present area, the period to travel to each gate of the current room, the projected interval from each gate to the exit, and the space already covered in the area. The agent replies vigorously to altering logjams, gate lead-ins/ends, and variations in area promptness restrictions. The user can modify the default parameter weights to change the behavior. For example, occupants can neglect queues and only look for the closest exit.

### 4.3 Result

Validation was done by comparing the evacuation time when the simulation was completed on the intelligent agent application and pathfinder application. Agents in the intelligent application are drawn as circles in the simulation while occupants in pathfinder are shown as upright cylinders on the movement mesh. The position and speed of both agents and occupants in intelligent and pathfinder are both specified in the simulation applications. Intelligent application has one simulation mode where agents steer themselves so they do not pass through other agents. This provides a more realistic movement seen in humans of collision detection and avoidance but it can lead to extreme queueing at the exits. Pathfinder has steer mode and also the SFPE mode where occupants are allowed to go through other occupants which provides an artificial movement but minimizes queueing at the exit.

Figure 8, average total shows the time taken by running the pathfinder application depicted as the blue bars and evacuation intelligent agent application depicted as the red bars. This simulation was done by increasing the numbers of occupants by ten starting from ten and going all the way up to seventy occupants in the simulation. The seventy number of occupants was chosen to match the maximum number of occupants that can fit in the computer lab in our department building. The Y-axis shows evacuation time and X-axis shows the number of occupants available during the simulation. The simulation was performed 50 times each using the pathfinder application and

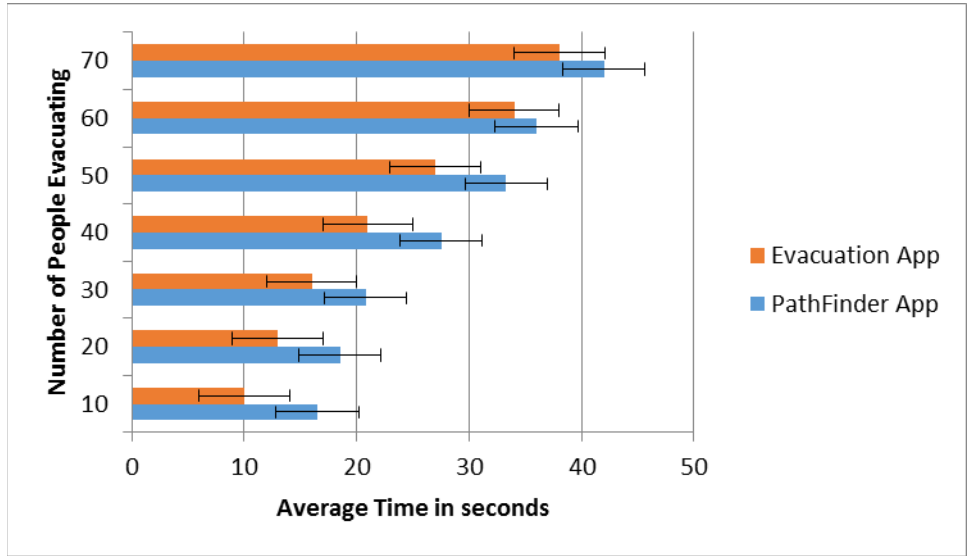


Figure 8: Average total run time error bar

evacuation intelligent agent application. As above in Figures 6 and 7, the occupants were placed randomly in the environment and all of them had the same speed of 1.19 pixels per sec. We took each run at the interval of ten, twenty, thirty, forty, fifty, sixty and seventy occupants. At each interval, we took average time of evacuation. The error bar on the bar graphs shows the variance in average time with standard error of fixed value 0.1, 95% confidence level and standard deviation 1.0. We can say that the more the number of occupants increased in the simulation, the more divergent the errors bars between the pathfinder application and the intelligent agent evacuation application. Our proposed C# evacuation application and the

pathfinder application both had similar functionality and performance that allowed them to be effective tools for data visualization in emergency evacuation. Figure 9 shows the error bar in the line graph of the comparison seen when running the intelligent agent application (red line) and the pathfinder application (blue line). The same interval of occupants starting at ten and going all the way up to seventy is shown in the line graph. The blue line representing the pathfinder application is shown with its error bar not intersecting with the error bar of the red line evacuation application at ten occupants. As the number of occupants increases in the simulation, it is shown that the error bars get

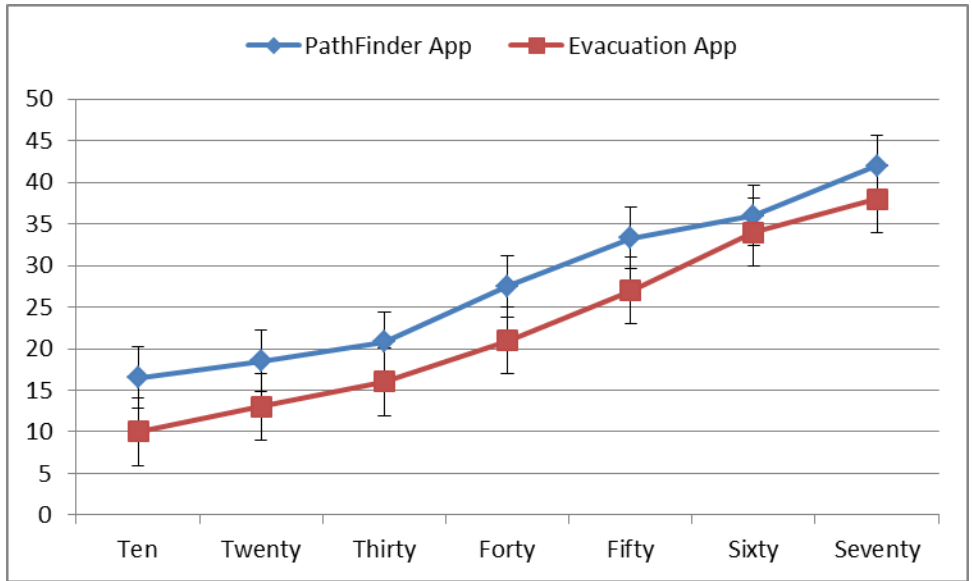


Figure 9: Average evacuation time with error line

closer until they intersect, showing that at seventy occupants the difference between both simulations are not statistically significant. It can be seen that at a lower number of occupants the evacuation application performs slightly better than the pathfinder application.

The average evacuation time was 10 seconds for evacuation application and 16.5 seconds for pathfinder application at ten occupants. Similarly, 13 seconds for evacuation application and 18.5 seconds for pathfinder application are recorded for twenty occupants. The average evacuation time was 16 seconds for evacuation application and 20.8 seconds for pathfinder application with thirty occupants. The rest of the evacuation time for forty, fifty, sixty and seventy occupants in evacuation application was 21, 27, 34 and 38 seconds, respectively. Similarly, for pathfinder application 27.5, 33.3, 36 and 42 seconds was recorded, respectively. Overall, the curve of pathfinder is going uphill the highest, which displays data that when the pathfinder algorithm is used, there is a slight increase in the evacuation time. According to the model, wait time of participants increases when more participants are trying to evacuate at the same time. This delay is seen in real life with participants becoming unpredictable when it comes to making decisions in emergencies. As a result, their behavior becomes erratic. At each interval, we took average time of evacuation. The error bar on bar graphs shows the difference in average time with 95% confidence level.

## 5 Conclusion

Our proposed C# application can be used to model situations that are difficult to test in real-life due to safety considerations. It is able to include agent characteristics and behaviors. The findings of this modeling are very encouraging as the agents are able to assume various roles to combine GA and NN on the way to reaching their goals. We hope our proposed tool will help in visualizing evacuation time and what-if scenarios for environments that are difficult to model in real life. It will also act as a training and educational tool for depicting different evacuation strategies and damage control decisions during evacuation. The proposed application will aid in running multiple evacuation drills for what-if scenarios by incorporating agent characteristics that can scale from a room, to a building, to a whole section of buildings in an area. The future work will involve the implementation of altruistic behavior and selfish behavior.

Future work will comprise of the usage of 3D applications such as Microsoft XNA using triangles or pixels finding their way to a goal in a 3D space. Examination of a 3D environment will make the prototype more in line with the real world and increase the ability to forecast link of vision to stop agents from running into each other in the environment. Feasibly estimating the route using likelihoods for mimicking agent centered actions and the situation where agents jump find their way in the environment by using 3D XNA and its physics libraries.

The use of 3D graphics and physics in a simulation involves

communication between Microsoft XNA tools and game engines and the C-Sharp .net executable. This communication can be performed by making calls to the Application Program Interface (API). The API is a group of procedures, conventions, and apparatuses for construction of software applications. The API stipulates by what method software modules ought to work together, and APIs are used when developing software for graphical user interface (GUI) modules. The contents that can be manipulated by the API calls to XNA include block images as obstacles, door images as exits and person images as agents in the simulation. Each of these objects can be rendered as a 3D texture and placed in a vector position in the environment. A sprite batch can be used to draw and visualize the texture, using the game engine graphics device. Obstacle avoidance can be done in the visual interface by calculating the vector to steer the agent away from the obstacle using certain thresholds, differentials and normalizing adjustment values. It is also possible to use keyboard state to manually control the up, down, left and right movement of an agent in the simulation. This can be a way for future work by a researcher interested in extending the simulator.

Actual records deliver valuable understanding and numerical data that will provide us the prospect to figure out numerous fascinating methodical matters regarding the construction and application of people performance simulations. Numerous diverse expertise have been investigated to spontaneously find persons and items for the Computer Science building at Bowie State University, Maryland. Video camera recording is one of the tools investigated, and it was discovered that it is effective in locating specific persons as they pass edges, such as the doors and exits to places or houses. Gathering actual records will be of enormous assistance to somebody who is fresh to the space and is forecasting to do additional examination.

Future work shall comprise expansion of additional activation functions. This may produce more analysis outcomes and application of genetic algorithm and neural networks actions. The additional examination with a genetic algorithm can also provide favorable consequences. Future work will be concentrated on creating the application's actions to be dynamic in the model of social agents. Autonomous agents and modification in the procedures and association utilities for the dynamic behavior might influence stimulating outcomes.

## Acknowledgments

This work is funded in part by the National Science Foundation grant number HRD-1238784 and DHS award 2011-ST-062-000050.

## References

- [1] L. Benthorn and H. Frantzich, "Fire Alarm in a Public Building: How do People Evaluate Information and Choose Evacuation Exit?" Dept. of Fire Safety Engineering, Lund University, 1996.

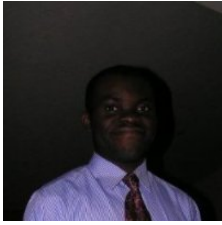
- [2] N. Chooramun, P. Lawrence, and E. Gale, "Implementing a Hybrid Space Discretisation Within an Agent Based Evacuation Model," PED 2010, NIST, Maryland USA, 2010.
- [3] E. Galea, "buildingEXODUS V6.0 User Guide and Technical Manual," Doc Rev 5.0, November 2013.
- [4] E. R. S. Gwynne, P. J. Lawrence, and L. (n.d.). Filippidis, "A Review of the Methodologies used in the Computer Simulation of Evacuation from the Built Environment," Fire Safety Engineering Group, Center for Numerical Modeling and Process Analysis, University of Greenwich, London, UK, 1999.
- [5] I. Millington and J. Funge, *Artificial Intelligence for Games*, Second Edition, Morgan Kaufmann Publishers, pp. 647, 2009.
- [6] K. Ogunlana and S. Sharma, "Agent Based Simulation Model for Data Visualization during Evacuation", Proceedings of 2014 ASE/IEEE BIGDATA/SOCIALCOM/CYBERSECURITY Conference, ISBN: 978-1-62561-000-3, Stanford University, pp. 1-6, May 27-31, 2014.
- [7] R. D. Peacock, J. D. Averill, and E. D. Kuligowski, "Stairwell Evacuation from Buildings: What We Know We Don't Know," National Institute of Standards and Technology, Gaithersburg, MD, 16, 2009.
- [8] T. T. Pires, "An Approach for Modeling Human Cognitive Behavior in Evacuation Models," *Fire Safety Journal*, 40(0379-7112):177-189, 2005.
- [9] L. S. Poon, "A Simulation Model of Occupants with Behavioral Attributes in Emergency Evacuation of High-Rise Building Fires," *Fire Safety Science-Proceedings of the Fourth International Symposium*, pp. 681-692, 1994.
- [10] M. J. Quinn, R. A. Metoyer, and K. (n.d.). Hunter-Zaworski, "Parallel Implementation of the Social Forces Model," School of Electrical Engineering and Computer Science Department of Civil, Construction, and Environmental Engineering, Oregon State University Corvallis, OR 97331 USA, 2003.
- [11] S. Russell and P. Norvig, *Artificial Intelligence a Modern Approach*, Prentice Hall Pearson Education, Inc, Second Edition, 116,526,632,736, 2003.
- [12] S. Sharma, "Avatarsim: A Multi-Agent System for Emergency Evacuation Simulation," *Journal of Computational Methods in Science and Engineering*, ISSN 1472-7978, 9(1,2):S13-S22, 2009.
- [13] S. Sharma, "Fuzzy Approach for Predicting Probability of Reaching a Target in a Battlefield Environment," *International Journal of Computers and their Applications*, 17(1):16-24, March 2010.
- [14] S. Sharma, "Use of Favorite Goal in Agent Based Modeling and Simulation\*," *IJCA*, 19(1):1-4, 2012.
- [15] S. Sharma and K. Ogunlana, "Using Genetic Algorithm and Neural Networks in a Goal Finding Application for Evacuation," Proceedings at the ISCA 22nd International Conference on Software Engineering and Data Engineering (SEDE-2013), Los Angeles, California, USA, pp. 25-30, Sep 25-27, 2013.
- [16] S. Sharma, S. Otunba, K. Ogunlana, and T. Tripathy, "Intelligent Agents in a Goal Finding Application for Homeland Security," Proceedings of the IEEE Southeast Conf, pp. 1, 2012.
- [17] S. Sharma, A. Singh, and H. Prakash, "Multi-Agent Modeling and Simulation of Human Behavior in Aircraft Evacuations," *IEEE Transactions on Aerospace and Electronic Systems*, 44(4):1477-1488, October 2008.
- [18] S. Sharma and H. Singh, "Multi-Agent System for Simulating Human Behavior in Egress Simulations," Proceedings of NAACOS, Annual Conference of the North American Association for Computational Social and Organizational Sciences, Notre Dame, Indiana, ISSN 1472-797, pp. 1-2, June 2006.
- [19] S. Sharma, H. Singh, and G. R. Gerhart, "Simulation of Convoy of Unmanned Vehicles using Agent Based Modeling," SPIE Conference on Security and Defense, Florence, Italy, 17-20 September 2007.
- [20] T. Shen and S. Chien, "An Evacuation Simulation Model (ESM) for Building Evaluation," Graduate School of Fire Science and Administration, Central Police University, *Taiwan International Journal on Architectural Science*, 6(1):15-30, 2005.
- [21] L. Shi, Q. Xie, X. Cheng, L. Chen, Y. Zhou, and R. (n.d.). Zhang, "Developing a Database for Emergency Evacuation Model, State Key Laboratory of Fire Science," University of Science and Technology of China, West Campus, Anhui, Hefei 230027, PR China, 2009.
- [22] "Simulex User Guide 6.0," Integrated Environmental Solutions Limited, 2012.
- [23] H. Winter, "Modeling Crowd Dynamics During Evacuation Situations Using Simulation," Lancaster University, 2012.
- [24] Q. Zhang, K. C. Gupta, and V. K. Devabhaktuni, "Artificial Neural Networks for RF and Microwave Design - from Theory to Practice," *IEEE Transactions Microwave Theory and Techniques*, doi: 10.1109/TMTT.2003.809179, 51(4):1339-1350, Apr 2003.



**Sharad Sharma** is an Associate Professor in the Department of Computer Science at the Bowie State University. He has received Ph.D in Computer Engineering from Wayne State University, Detroit, MI in 2006 and M.S. from University of Michigan, Ann Arbor, MI in 2003. He has won

the "Outstanding Researcher Award" in year 2013 and 2011, "Outstanding Faculty Award" in year 2012, "Outstanding Publication Award" in year 2010, and "Outstanding Young Faculty Award" in year 2009 at College of Arts and Science in

the Bowie State University. Dr. Sharma is the Director of the Virtual Reality Laboratory at the Bowie State University. The laboratory applies virtual reality and augmented reality as a tool for learning, training, and education. Dr. Sharma's research focus is on modeling and simulation of multi-agent systems for emergency scenarios. His work is motivated by the need of research in real-time agent navigation for reaching a goal in emergency situations like evacuation.



**Kolawole Ogunlana** will be receiving his PhD from the Department of Computer Science at the Bowie State University on December 2015. He has received M.S. in Computer Science from Catholic University of America (CUA) in 2006 and B.S. from University of Maryland, College Park in 2003. He has won published many papers under Dr. Sharma at College of Arts and Science in the Bowie State University. Kola's research focus is on modeling and simulation of multi-agent systems for emergency scenarios especially in a building. His work is motivated by the need of research in real-time agent navigation for reaching a goal in emergency situations like evacuation saving time and money.

## Index

### Authors

#### A

- Abdul, Wahab**, see Yaacob, Hamwira; *IJCA v22 n1 March 2015 31-42*
- Ali, Zulfiqar**, Ghulam Muhammad, Mansour Alsulaiman, Irraivan Elamvazuthi, and Khalid Al-Mutib; Oriented and Interpolated Local Features for Speech Recognition of Vocal Fold Disordered Patients; *IJCA v22 n1 March 2015 3-11*
- Aljahdali, Sultan**, see Buragga, Khalid A.; *IJCA v22 n3 Sept 2015 137-145* *IJCA v22 n4 Dec 2015 164-171*
- Al-Mutib, Khalid**, see Ali, Zulfiqar; *IJCA v22 n1 March 2015 3-11*
- Al Na'mneh** and Khalid A. Darabkh; New Superfast Bit Reversal Algorithms on Uniprocessors; *IJCA v22 n4 Dec 2015 147-156*
- Alodib, Mohammed**; An Analytical Approach for the Enhancement of Services Provided using Big Data Technique; *IJCA v22 n2 June 2015 75-86*
- Alsulaiman, Mansour**, see Ali, Zulfiqar; *IJCA v22 n1 March 2015 3-11*

#### B

- Bahney, Chelsea**, see Marmor, Meir; *IJCA v22 n2 June 2015 51-58*
- Bossard, Antoine** and Keiichi Kaneko; A Node-to-Set Disjoint Paths Routing Algorithm in Torus-Connected Cycles; *IJCA v22 n1 March 2015 22-30*
- Buragga, Khalid A.**, Sultan Aljahdali, and E. A. Zanaty; Improving Fuzzy C-Means Algorithm for Magnetic Resonance Images (MRIs) Segmentation; *IJCA v22 n3 Sept 2015 137-145*
- Buragga, Khalid A.**, Sultan Aljahdali, Ahmad. M. Sarhan, and Marcel Karam; A Personal Identification System Based on Iris Recognition; *IJCA v22 n4 Dec 2015 164-171*

### C-G

- Chishiro, Hiroyuki** and Nobuyuki Yamasaki; Zero-Jitter Semi-Fixed-Priority Scheduling with Harmonic Periodic Task Sets; *IJCA v22 n3 Sept 2015 119-127*
- Chishiro, Hiroyuki**, see Mizotani, Keigo; *IJCA v22 n3 Sept 2015 128-136*
- Darabkh, Khalid A.**, see Al Na'mneh; *IJCA v22 n4 Dec 2015 147-156*
- Elamvazuthi, Irraivan**, see Ali, Zulfiqar; *IJCA v22 n1 March 2015 3-11*
- Etschmaier, Maximilian**; Purposeful Systems: A Conceptual Framework for System Design, Analysis, and Operation; *IJCA v22 n2 June 2015 87-99*
- Falade, A. J.**; A Study of the Performance of Diversity Combining Schemes on Multipath Fading at 900MHZ; *IJCA v22 n4 Dec 2015 157-163*
- Gupta, Bidyut**, Sindooru Koneru, and Shahram Rahimi; LSR-Based Core Selection in Shared Tree Multicasting; *IJCA v22 n1 March 2015 12-21*

### H-J

- Hatori, Yusuke**, see Mizotani, Keigo; *IJCA v22 n3 Sept 2015 128-136*
- Hunt, C. Anthony**, see Marmor, Meir; *IJCA v22 n2 June 2015 51-58*
- Iwasaki, Hirotoshi**, see Nishiyama, Hiroyuki; *IJCA v22 n3 Sept 2015 110-118*
- Koneru, Sindooru**, see Gupta, Bidyut; *IJCA v22 n1 March 2015 12-21*

### K-L

- Kamaruddin, Norhaslinda**, see Yaacob, Wahab; *IJCA v22 n1 March 2015 31-42*
- Kaneko, Keiichi**, see Bossard, Antoine; *IJCA v22 n1 March 2015 22-30*

- Karam, Marcel**, see Buragga, Khalid A.; *IJCA v22 n4 Dec 2015 164-171*
- Kumura, Yusuke**, see Mizotani, Keigo; *IJCA v22 n3 Sept 2015 128-136*
- Le, Dien Tuan**, Minjie Zhang, Fenghui Ren, and Xudong Luo; A Regression-Based Approach for Threshold Selections of Support and Confidence in Association Rule Mining; *IJCA v22 n2 June 2015 59-74*
- Luo, Xudong**, see Le, Dien Tuan; *IJCA v22 n2 June 2015 59-74*

### M-R

- Marcucio, Ralph**, see Marmor, Meir; *IJCA v22 n2 June 2015 51-58*
- Marmor, Meir**, Ralph Marcucio, Chelsea Bahney, and C. Anthony Hunt; Mechanistically Explanatory Biomimetic Analogs for Fracture Healing; *IJCA v22 n2 June 2015 51-58*
- Mizoguchi, Fumio**, see Nishiyama, Hiroyuki; *IJCA v22 n3 Sept 2015 110-118*
- Mizotani, Keigo**, Yusuke Hatori, Yusuke Kumura, Masayoshi Takasu, Hiroyuki Chishirao, and Nobuyuki Yamasaki; An Intergation of Imprecise Computation Model and Real-Time Voltage and Frequency Scaling on Responsive Multithreaded Processor; *IJCA v22 n3 Sept 2015 128-136*
- Muhammad, Ghulam**, see Ali, Zulfiqar; *IJCA v22 n1 March 2015 3-11*
- Nishiyama, Hiroyuki**, Akira Yoshizawa, Hirotoshi Iwasaki, and Fumio Mizoguchi; Design and Implementation of a New Tool for Detecting Distracted Car Driving Using Eye Movement and Driving Data on a Tablet PC; *IJCA v22 n3 Sept 2015 110-118*
- Ogunlana, Kolawole**, see Sharma Sharad; *IJCA v22 n4 Dec 2015 172-182*
- Peyravi, Hassan**, see Sehgal, Rahul; *IJCA v22 n3 Sept 2015 102-109*

**Ren, Fenghui**, see Le, Dien Tuan; *IJCA v22 n2 June 2015 59-74*

### S-V

**Sarhan, Ahmad. M.**, see Buragga, Khalid A.; *IJCA v22 n4 Dec 2015 164-171*

**Sehgal, Rahul** and Hassan Peyravi; End to End Delay Analysis in Delay Tolerant Networks; *IJCA v22 n3 Sept 2015 102-109*

**Sharma, Sharad** and Kolawole Ogunlana; Using Genetic Algorithm & Neural Network for Modeling Learning Behavior in a Multi-Agent System during Emergency Evacuation; *IJCA v22 n4 Dec 2015 172-182*

**Shi, Yong**; An Approach to Dynamically Adjusting Clusters and Outliers for Multi-Dimensional Data Sets; *IJCA v22 n1 March 2015 43-50*

**Takasu, Masayoshi**, see Mizotani, Keigo; *IJCA v22 n3 Sept 2015 128-136*

### W-Z

**Yaacob, Hamwira**, Wahab Abdul, and Norhaslinda Kamaruddin; CMAC-Based Computational Model of Affects (CCMA) from Self-Organizing Feature Mapping Weights for Classification of Emotion Using EEG Signals; *IJCA v22 n1 March 2015 31-42*

**Yamasaki, Nobuyuki**; see Chishiro, Hiroyuki; *IJCA v22 n3 Sept 2015 119-127*

**Yamasaki, Nobuyuki**, see Mizotani, Keigo; *IJCA v22 n3 Sept 2015 128-136*

**Yoshizawa, Akira**, see Nishiyama, Hiroyuki; *IJCA v22 n3 Sept 2015 110-118*

**Zanaty, E. A.**, see Buragga, Khaid A.; *IJCA v22 n3 Sept 2015 137-145*

**Zhang, Minjie**, see Le, Dien Tuan; *IJCA v22 n2 June 2015 59-74*

**Key Words****A**

**Affective computing**  
*IJCA v22 n1 March 2015 31-42*

**Agent-based evacuation**  
*IJCA v22 n4 Dec 2015 172-182*

**Automatic speech recognition**  
*IJCA v22 n1 March 2015 3-11*

**Arabic digits**  
*IJCA v22 n1 March 2015 3-11*

**Arousal**  
*IJCA v22 n1 March 2015 31-42*

**Artificial neural network (ANN)**  
*IJCA v22 n4 Dec 2015 164-171*

**Association rule mining**  
*IJCA v22 n2 June 2015 59-74*

**B-C**

**Big data**  
*IJCA v22 n2 June 2015 75-86*

**Biometrics**  
*IJCA v22 n4 Dec 2015 164-171*

**Bit error rate**  
*IJCA v22 n4 Dec 2015 157-163*

**Bit-reversal**  
*IJCA v22 n4 Dec 2015 147-156*

**Bone healing**  
*IJCA v22 n2 June 2015 51-58*

**Cerebellar model of articulation controller (CMAC)**  
*IJCA v22 n1 March 2015 31-42*

**Cloud computing**  
*IJCA v22 n2 June 2015 75-86*

**Clusters**  
*IJCA v22 n1 March 2015 43-50*

**Cognitive distraction**  
*IJCA v22 n3 Sept 2015 110-118*

**Confidence**  
*IJCA v22 n2 June 2015 59-74*

**Coordination**  
*IJCA v22 n2 June 2015 75-86*

**Core selection**  
*IJCA v22 n1 March 2015 12-21*

**D**

**Data mining**  
*IJCA v22 n1 March 2015 43-50*

**Delay analysis**  
*IJCA v22 n3 Sept 2015 102-109*

**Delay/disruption tolerant networks**  
*IJCA v22 n3 Sept 2015 102-109*

**Designer education**  
*IJCA v22 n2 June 2015 87-99*

**Designer qualifications**

*IJCA v22 n2 June 2015 87-99*

**Detecting distracted car driving**  
*IJCA v22 n3 Sept 2015 110-118*

**Diversity combining**  
*IJCA v22 n4 Dec 2015 157-163*

**Driving data**  
*IJCA v22 n3 Sept 2015 110-118*

**Dynamics data sets**  
*IJCA v22 n1 March 2015 43-50*

**E-F**

**Embedded real-time systems**  
*IJCA v22 n3 Sept 2015 128-136*

**Emergency evacuation**  
*IJCA v22 n4 Dec 2015 172-182*

**Encephalogram (EEG)**  
*IJCA v22 n1 March 2015 31-42*

**Evolution**  
*IJCA v22 n2 June 2015 87-99*

**Evolving fuzzy neural network (EFuNN)**  
*IJCA v22 n1 March 2015 31-42*

**Eye movement**  
*IJCA v22 n3 Sept 2015 110-118*

**Fast Fourier transforms**  
*IJCA v22 n4 Dec 2015 147-156*

**Fault-tolerant routing**  
*IJCA v22 n1 March 2015 22-30*

**Feature extraction**  
*IJCA v22 n4 Dec 2015 164-171*

**Fuzzy clustering**  
*IJCA v22 n3 Sept 2015 137-145*

**G-H**

**Genetic algorithm**  
*IJCA v22 n4 Dec 2015 172-182*

**Harmonic periodic task sets**  
*IJCA v22 n3 Sept 2015 119-127*

**Hierarchy transpose**  
*IJCA v22 n4 Dec 2015 147-156*

**HMM**  
*IJCA v22 n1 March 2015 3-11*

**I-J**

**Imprecise computation**  
*IJCA v22 n3 Sept 2015 119-127*

**Imprecise computation model**  
*IJCA v22 n3 Sept 2015 128-136*

**In Silico**  
*IJCA v22 n2 June 2015 51-58*

**Insight**  
*IJCA v22 n2 June 2015 87-99*

**Interconnection network**

*IJCA v22 n1 March 2015 22-30*

**Iris**  
*IJCA v22 n4 Dec 2015 164-171*

**Jitter**  
*IJCA v22 n3 Sept 2015 119-127*

**K-L**

**Link intermittency**  
*IJCA v22 n3 Sept 2015 102-109*

**Link state routing**  
*IJCA v22 n1 March 2015 12-21*

**M**

**Markov chains**  
*IJCA v22 n3 Sept 2015 102-109*

**Mean connection time**  
*IJCA v22 n3 Sept 2015 102-109*

**Mechanisms**  
*IJCA v22 n2 June 2015 51-58*

**Medical image segmentation**  
*IJCA v22 n3 Sept 2015 137-145*

**MFCC**  
*IJCA v22 n1 March 2015 3-11*

**Model driven architecture**  
*IJCA v22 n2 June 2015 75-86*

**Models**  
*IJCA v22 n4 Dec 2015 172-182*

**Modified fuzzy c-means**  
*IJCA v22 n3 Sept 2015 137-145*

**Multi-dimensional data**  
*IJCA v22 n1 March 2015 43-50*

**Multicomputer**  
*IJCA v22 n1 March 2015 22-30*

**Multipath fading**  
*IJCA v22 n4 Dec 2015 157-163*

**Multi-perception**  
*IJCA v22 n4 Dec 2015 172-182*

**Multiple correlation coefficients**  
*IJCA v22 n2 June 2015 59-74*

**N-O**

**Neuro network**  
*IJCA v22 n4 Dec 2015 172-182*

**Neuroscience**  
*IJCA v22 n2 June 2015 87-99*

**Outlier detection**  
*IJCA v22 n1 March 2015 43-50*

**P-Q**

**Parallel processing**  
*IJCA v22 n1 March 2015 22-30*

**Performance analysis**  
*IJCA v22 n4 Dec 2015 147-156*

**Performance evaluation***IJCA v22 n1 March 2015 22-30***Power consumption***IJCA v22 n3 Sept 2015 128-136***Pseudo sub-diameter***IJCA v22 n1 March 2015 12-21***Purposeful system***IJCA v22 n2 June 2015 87-99***Vocal fold disorders***IJCA v22 n1 March 2015 3-11***Wavelets***IJCA v22 n4 Dec 2015 164-171***Web services***IJCA v22 n2 June 2015 75-86***R****Rahimi, Shahram**, see Gupta, Bidyut;*IJCA v22 n1 March 2015 12-21***Rayleigh channel***IJCA v22 n4 Dec 2015 157-163***Regression model***IJCA v22 n2 June 2015 59-74***Response multithreaded processor***IJCA v22 n3 Sept 2015 128-136***RT-VFS***IJCA v22 n3 Sept 2015 128-136***S****Schedulability***IJCA v22 n3 Sept 2015 119-127***Semi-fixed-priority scheduling***IJCA v22 n3 Sept 2015 119-127***Shared tree***IJCA v22 n1 March 2015 12-21***Super pseudo sub-diameter***IJCA v22 n1 March 2015 12-21***Support***IJCA v22 n2 June 2015 59-74***Swapping algorithms***IJCA v22 n4 Dec 2015 147-156***System analysis***IJCA v22 n2 June 2015 87-99***System design***IJCA v22 n2 June 2015 87-99***System operation***IJCA v22 n2 June 2015 87-99***T-Z****Tablet PC***IJCA v22 n3 Sept 2015 110-118***Tandem queues***IJCA v22 n3 Sept 2015 102-109***Time complexity***IJCA v22 n4 Dec 2015 147-156***Valence***IJCA v22 n1 March 2015 31-42***Vector quantization (VQ)***IJCA v22 n4 Dec 2015 164-171***Virtual experimentation***IJCA v22 n2 June 2015 51-58*

# Instructions For Authors

---

The International Journal of Computers and Their Applications is published multiple times a year with the purpose of providing a forum for state-of-the-art developments and research in the theory and design of computers, as well as current innovative activities in the applications of computers. In contrast to other journals, this journal focuses on emerging computer technologies with emphasis on the applicability to real world problems. Current areas of particular interest include, but are not limited to: architecture, networks, intelligent systems, parallel and distributed computing, software and information engineering, and computer applications (e.g., engineering, medicine, business, education, etc.). All papers are subject to peer review before selection.

---

## A. Procedure for Submission of a Technical Paper for Consideration

1. Email your manuscript to the Editor-in-Chief, Dr. Fred Harris, Jr., Fred.Harris@cse.unr.edu.
2. Illustrations should be high quality (originals unnecessary).
3. Enclose a separate page (or include in the email message) the preferred author and address for correspondence. Also, please include email, telephone, and fax information should further contact be needed.

## B. Manuscript Style:

1. The text should be **double-spaced** (12 point or larger), **single column** and **single-sided** on 8.5 X 11 inch pages.
2. An informative abstract of 100-250 words should be provided.
3. At least 5 keywords following the abstract describing the paper topics.
4. References (alphabetized by first author) should appear at the end of the paper, as follows: author(s), first initials followed by last name, title in quotation marks, periodical, volume, inclusive page numbers, month and year.
5. Figures should be captioned and referenced.

## C. Submission of Accepted Manuscripts

1. The final complete paper (with abstract, figures, tables, and keywords) satisfying Section B above in **MS Word format** should be submitted to the Editor-in-Chief.
2. The submission may be on a CD/DVD or as an email attachment(s) . **The following electronic files should be included:**
  - Paper text (required).
  - Bios (required for each author). Integrate at the end of the paper.
  - Author Photos (jpeg files are required by the printer, these also can be integrated into your paper).
  - Figures, Tables, Illustrations. These may be integrated into the paper text file or provided separately (jpeg, MS Word, PowerPoint, eps).
3. Specify on the CD/DVD label or in the email the word processor and version used, along with the title of the paper.
4. Authors are asked to sign an ISCA copyright form (<http://www.isca-hq.org/j-copyright.htm>), indicating that they are transferring the copyright to ISCA or declaring the work to be government-sponsored work in the public domain. Also, letters of permission for inclusion of non-original materials are required.

## Publication Charges

After a manuscript has been accepted for publication, the contact author will be invoiced for publication charges of **\$50.00 USD** per page (in the final IJCA two-column format) to cover part of the cost of publication. For ISCA members, \$100 of publication charges will be waived if requested.

